NASA TM X- 63233

10.6-MICRON LASER COMMUNICATIONS SYSTEM EXPERIMENT FOR ATS-F AND ATS-G

NELSON McAVOY
HERBERT L. RICHARD
JOHN H. McELROY
WILLIAM E. RICHARDS

MAY 1968

JUN 1968

RECEIVED
NASA STI FACILITY

GSFC —— **GODDARD SPACE FLIGHT CENTER** ——

GREENBELT, MARYLAND

10.6-MICRON LASER COMMUNICATIONS SYSTEM EXPERIMENT

FOR ATS-F AND ATS-G

Nelson McAvoy
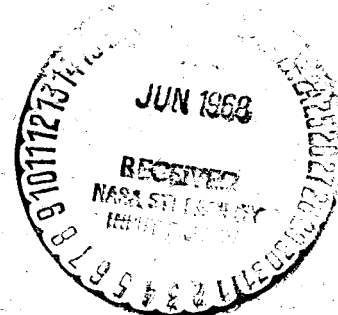Herbert L. Richard
John H. McElroy
William E. Richards

Advanced Development Division

May 1968

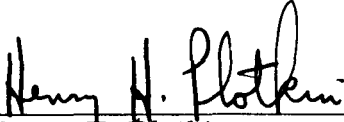GODDARD SPACE FLIGHT CENTER
Greenbelt, Maryland

10.6-MICRON LASER COMMUNICATIONS SYSTEM EXPERIMENT

FOR ATS-F AND ATS-G

Nelson McAvoy
Herbert L. Richard
John H. McElroy
William E. Richards

Advanced Development Division
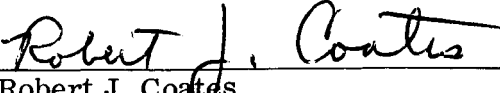
May 1968

Approved:

_____
Henry H. Plotkin
Head, Optical Systems Branch

_____
Victor R. Simas
Head, RF Systems Branch

_____
Robert J. Coates
Chief, Advanced Development Division

GODDARD SPACE FLIGHT CENTER
Greenbelt, Maryland

ABSTRACT

The purpose of the coherent laser satellite-to-satellite experiment proposed for the ATS-F and -G program is to use the present laser state-of-the-art to establish the feasibility and value of optical space communications. Identical 23-pound tranceivers will be placed on ATS-F and -G, each consuming 20 watts of prime power. Information will be imposed on a frequency-modulated 10.6-micron carbon-dioxide laser beam within a 30-MHz bandwidth. A superheterodyne receiver with a 12.6-db noise figure will be used at each end of the link. A 5-inch-aperture optical antenna with a 100-db antenna gain and a 400-mw carrier, will provide a 28-db signal-to-noise ratio.

The experiment, incorporating components and subsystems tested in the laboratory and field, will be the first complete laser space-communications link. By establishing the above-mentioned weight, power levels, signal-to-noise ratio, and bandwidth, and by testing its performance in actual space operation, the engineering parameters necessary to meet NASA requirements for future applications to deep-space distances or for earth-orbital missions with information capacity far greater than the 30 MHz proposed here can be realistically predicted. A single 5-inch viewing port through the skin of the 30-foot antenna, used for both transmitting and receiving, will not interfere with the structure of the antenna pattern. Optical auto-tracking, sufficiently accurate to benefit from the intrinsic high gain of the optical antenna, will supplement pointing of the optical axis with respect to the ATS geostabilization.

As ATS-F and -G plans become more specific, the experiment may be integrated into other communications links: for example, S-band from Nimbus to ATS-G; 10.6 microns from ATS-G to ATS-F; and X-band from ATS-F to a data-acquisition facility. This approach to the ATS-F and -G program will pave the way for an operational integrated orbital network. It will provide baseline design information on the use of an optical link in the planned Data Relay Satellite (DRS) and the Earth Resources Technology Satellite series (ERTS).

The experiment will be conducted in two phases: the first, establishment of an optical data link between ATS-F and a ground terminal, will fulfill most of the technical objectives. It includes the use of a mobile laser ground station whose equipment will be essentially a prototype of the ATS-G flight package. The second phase will be to establish a high data-rate optical link between ATS-F and -G.

CONTENTS

CONTENTS (Continued)

ILLUSTRATIONS

ILLUSTRATIONS (Continued)

LIST OF TABLES

10.6-MICRON LASER COMMUNICATIONS SYSTEM EXPERIMENT

FOR ATS-F AND -G

Nelson McAvoy, Herbert L. Richard,
John H. McElroy, and William E. Richards
Advanced Development Division

1. INTRODUCTION

The purpose of the coherent wide-bandwidth spacecraft-to-spacecraft-to-ground laser communications experiment proposed for the ATS-F and -G program is to use the present laser state-of-the-art to establish the feasibility and value of optical communications. The experiment will require implementation and testing of a highly efficient wide-bandwidth high data-rate communications link between the ground and ATS-F and between two geosynchronous satellites, ATS-F and ATS-G. The chosen spectral range, 10.6 microns, offers optimum channel capacity per pound of satellite weight and satellite power budget.

The proposed experiment combines GSFC's capability in relay satellites—the technology of geosynchronizing and stabilizing ATS-F and -G orbits—with recent developments in laser communications to provide high-quality transmission from ATS-F to a small, portable laser-receiving station. The simplicity of the proposed ATS-F and -G flight packages, the use of laboratory-proven components, and the use of existing NASA facilities establish confidence that the experiment goals will be achieved, contingent only upon the normal performance of critical spacecraft subsystems. A high data-rate communications system at 10.6 microns ($28 \text{ tHz} = 28 \times 10^{12}$ Hz) has been realized over a long ground link (Reference 1).

The experiment will include its own telescope and steerable reflector. This 5-inch-diameter optical antenna will beam through a small hole in the skin of the 30-foot antenna from within the aft module (Figure 1). The experiment must be placed so that its line-of-sight toward the earth and to ATS-G is unobstructed.

The incidence on the satellite of laser radiation received from the earth can be kept as low as 10^{-13} watts per square centimeter throughout the communications experiment; consequently, it will not interfere with infrared equipment in the earth-viewing module (EVM) used for horizon sensing.

1

ATS-G

EQUATORIAL ORBIT PLANE

ATS-F
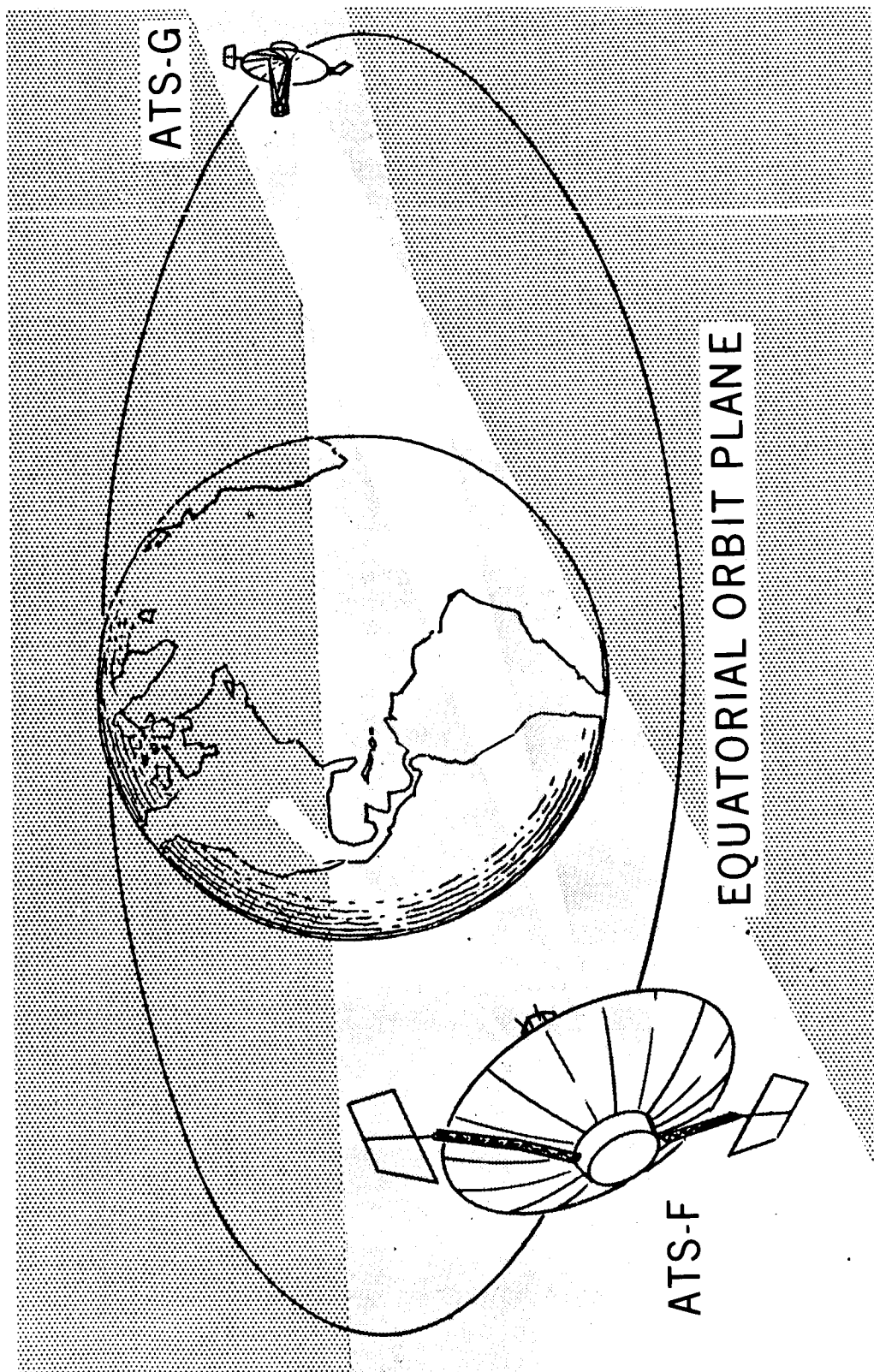
Figure 1. Laser Communication Link Geometry

The objectives of the experiment are as follows:

- Establish the feasibility of high data-rate 10.6-micron laser satellite-to-satellite communications and evaluate operational performance

- Provide baseline data necessary to design satellite-to-satellite optical links for the Data Relay Satellite and deep-space probes

- Provide information to directly compare microwave and infrared laser systems

- Provide 30-MHz wide, clear-weather, backup channels between ATS-F and the earth

- Provide 30-MHz wide, earth-to-earth, real-time, all-weather channels via ATS-F and -G, using both X-band and infrared links

The experiment will perform the following functions:

- Measure overall communication parameters, such as signal-to-noise ratio, bit-error rate, and system efficiency

- Measure laser transmitter frequency stability and drift under space environment

- Establish interrelation between receiver-noise bandwidth and laser local oscillator automatic frequency control (LO AFC) loop and its dependence on space-borne laser-frequency stability and Doppler shift

- Measure the noise figure of radiation-cooled infrared detectors/mixers in space

- Measure background noise presented to the infrared coherent receiver antenna when pointing at the earth, the sun, and other planets (Spikes in the background frequency spectrum-similar to the 1420-MHz hydrogen line-may occur in the 10-micron region.)

- Measure telescope-tracking servoloop parameters

Laser communications systems and components, and techniques of optical tracking, have reached the state of development necessary for this proposed experiment, in large part through the optical technology program carried out at NASA centers under direction of Headquarters' Office of Advanced Research and Technology. Pertinent tasks in progress at GSFC under this program are:

3

- 524-125-22-02-03-51, Stabilized CO_2 Laser

- 524-125-22-02-07-51, Coherent Optical Receiver Studies

- 524-125-22-02-12-51, Optical Instrumentation Development

- 524-125-22-02-24-51, Spacecraft Infrared Retroreflector

- 524-125-22-02-31-51, 10.6-Micron Satellite Experiments

- 524-125-22-02-32-51, Photon-Phonon Interaction Studies

- 524-125-22-02-34-51, 10-Micron Detector Field Package

- 524-125-21-02-09-51, 10.6-Micron D.C. Biased Optical Mixers

- 523-125-21-02-27-51, Laser Modulation

The following table lists the salient specifications for the proposed laser communications system. The first set of parameters relates to the system described in the succeeding sections; the second pertains to a less elaborate alternative system.

Communications System Parameters

Carrier frequency	28 tHz (10.6 micron)
Modulation mode	FM
System bandwidth	30 MHz
Modulation bandwidth	15 MHz
Antenna aperture	5 in.
Antenna gain	100 db
Prime power required	20 w
Mass	23 lb
Minimum detectable signal per Hz bandwidth	-160 dbm
Intermediate frequency	20 MHz
LO power	50 mw
Transmitter power	400 mw
Transmitter efficiency	8%
Signal-to-noise ratio at optical mixer	28 db
Range	3×10^7 meters
Atmospheric	4 db
Beam splitter loss	6 db

Optional System Parameters

Modulation bandwidth	5 MHz
Prime power required	20 w
Minimum detectable signal per Hz bandwidth	-160 dbm
Intermediate frequency	20 MHz
LO power	50 mw
Transmitter power	400 mw
Signal-to-noise ratio at optical mixer	36 db

2. EXPERIMENT DESCRIPTION

As stated previously, the overall objective of the 10.6-micron laser communication experiment is to establish the feasibility of a wide-bandwidth laser communication link between satellites. The experiment will be conducted in two phases: The first phase, establishing a high data-rate link between ATS-F and a ground terminal, will fulfill most of the experiment objectives; the second phase will establish the high data-rate link between satellites ATS-F and -G. Most of the technology required to provide a satellite-to-satellite laser communication link can be demonstrated by the first phase. Although ATS-G will not fly until approximately 1 year later, the ATS-F systems are designed to be operational when ATS-G is in orbit. Satellite lifetimes, which now average 2 years, are expected to increase to 3 or 3.5 years in the 1972 to 1973 period (Reference 2).

The laser communication link will then be established between ATS-F and ATS-G by "cross-strapping" the laser communications signals to the satellite-to-ground radio-frequency (RF) link. Similarly, the RF signals will be impressed on the laser communications link. The cross-strapping of signals will thus provide for the implementation of a real-time data-relay link from a low-orbiting satellite to ATS-G via radio, from ATS-G to -F by laser, and finally from ATS-F to a ground-based data-acquisition facility (DAF) via RF. This multifunction communications capability, shown in Figure 2, is a prototype of the operational functions required of the DRS.

The laser optical communication equipment consists of two basic parts: two flight packages, and the operational ground equipment.
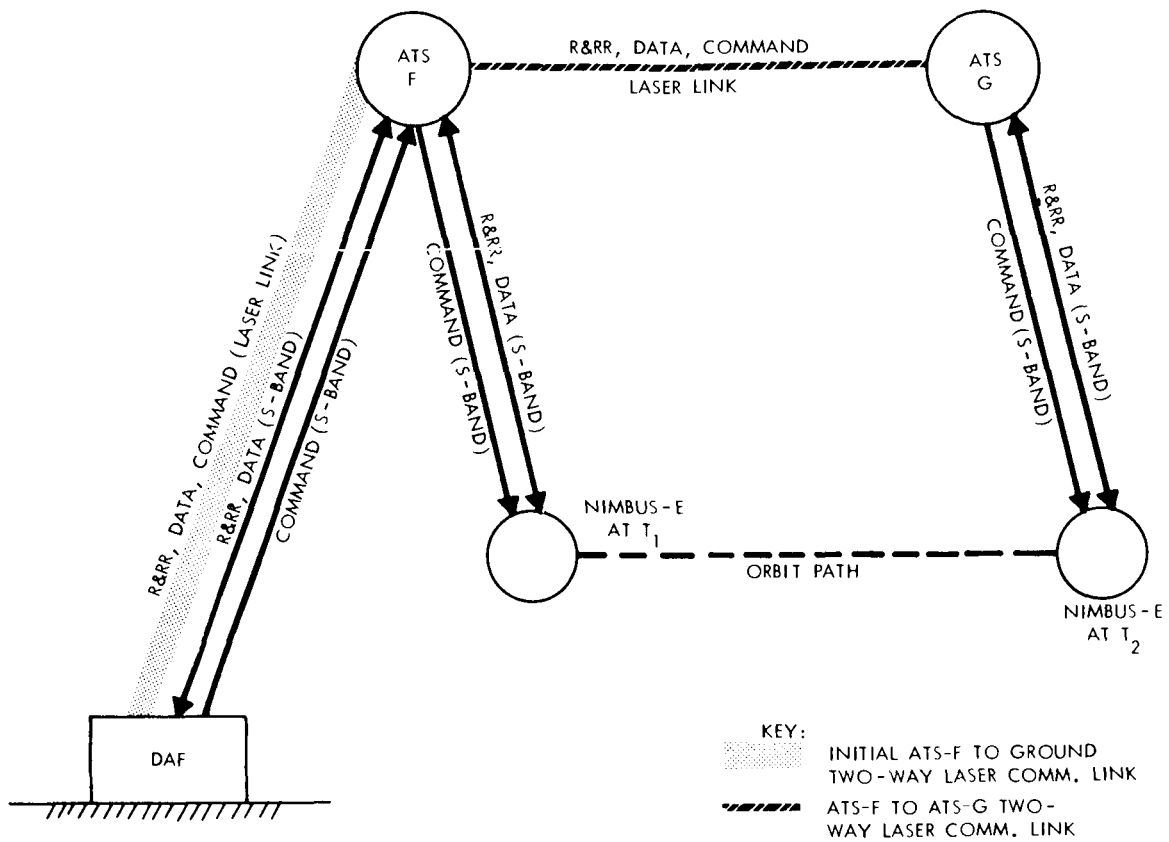
Figure 2. Multifunction Communication Capacity

3. FLIGHT PACKAGE

The flight package consists of five parts:

- The optical subsystem contains a coarse beam-pointing mechanism (slewing mirror), a 5-inch Cassegrainian telescope, image-motion compensator, directive mirrors, and beam splitters.

- The laser subsystem contains the 400-mw laser transmitter and modulator, the 50-mw laser local oscillator, the frequency-stabilization servo, and laser power meters.

- The detector subsystem contains the signal information detector, detector preamplifiers, image-motion detector, and radiation cooler.

- The signal-processing subsystem contains the intermediate frequency (IF) post amplifier, image-motion compensator drive electronics, laser transmitter modulator drive electronics, laser frequency-control electronics, beam-pointing mechanism drive electronics, and command and telemetry interface electronics.

- The power-supply subsystem contains the laser high-voltage and modulator power supplies and the low-voltage signal-processing and drive-electronics power supplies.

Table I shows weight and power budget for the proposed flight package.

3.1 OPTICAL SUBSYSTEM

The optical subsystem (Figure 3) is designed to scan the transmitted beam and receiver over the acquisition field-of-view, form a narrow transmitted beam, collect energy in the infrared portion of the spectrum, divide it between image-motion sensor and information detector, and superimpose local oscillator and received radiation to produce heterodyne action.

3.1.1 COARSE BEAM-POINTING MECHANISM

The coarse beam-pointing mechanism serves to direct the transmitted modulated beam toward the earth-based terminal as well as to direct the received laser signal into the Cassegrainian telescope. In the initial phase, the coarse beam-pointing mechanism on ATS-F will be positioned by command to point to any ground station within the continental United States. In the latter phase, it will be positioned to point to the ATS-G satellite which, for an equatorial tri-satellite position, would be displaced from the symmetry axis by ±30 degrees. This requires moving the coarse-pointing mirror over a 5-degree range in the north-south direction, and 30 degrees east-west. To effect a desired angular movement in the laser beam, the mirror has to move only half as much. Therefore, to position the mirror within the ±0.1-degree satellite-stabilization uncertainty, a 50-position resolver is required in the north-south, or Y-axis, direction and a 300-position resolver in the east-west, or X-axis, direction.

The bearing on the 5-inch coarse-pointing mirror will not experience much motion during the satellite lifetime. Only a few ground sites will be used, and ATS-G will be in a fixed position relative to ATS-F. After acquisition, corrections to the beam direction will be accomplished by a fine-control mechanism; therefore, very little repetitive positional movement is required of the coarse beam-pointing mechanism. Nevertheless, care will be exercised to provide the proper bearing lubrication for the mirror movement. For instance, vapor

7

Table 1
Proposed Weight and Power Budget

Components	Weight (lb)	Dimensions (in.)	Power (watts)
Optical Subsystem			
Beam-pointing mechanism	4.1	6×7×7	N/A
Telescope and structure	2.1	5×5×6	
Image-motion compensator	0.5	2×2×1.5	
Other optics	0.5	1 cm aperture	
Fixtures	1.0	N/A	
Subtotal	8.2	6×7×15	
Laser Subsystem			
Transmitter head	2.4	2×2×11	5
LO head	1.7	2×2×8	1
Subtotal	4.1	3×5×12	6
Detector Subsystem			
Radiation cooler (including detectors and preamplifiers)	0.9	6×6×3	
Subtotal	0.9	6×6×3	
Signal Processing Subsystem			
Signal detector amplifiers	0.25	1×1×1.3	0.4
Beam-pointing mechanism electronics	0.25	1×2×2	0.3
Angle sensor preamplifier	0.20	1/2×1/2×1/4	0.1
Angle sensor electronics	0.5	1×2×2	0.4
Image motion compensator electronics	0.5	1×2×2	2.0
Modulator drive	0.5	1/4×1/2×1	1.0
Command and telemetry interface	0.5	1×2×3	1.0
Laser AFC	0.4	1×2×2	.4
Subtotal	3.1	4×6×6	5.6
Power Supply Subsystem			
Transmitter	0.125	1×3×3	4.0
LO	0.125	1×2×3	1.0
Modulator	0.125	1×2×3	2.7
Beam-pointing mechanism	0.250	1×2×3	0.1
Image-motion compensator	0.250	1×2×3	0.10
Detector	0.125	1×1×1	0.10
Signal processor	0.250	1×1×1	0.4
Subtotal	1.25	4×6×6	8.4
Components subtotal	17.6	Max. 8×6×6 Max. 22×17×7-3/4	20.0
Misc. structure	5.0		
TOTAL	22.6	Max. 8×6×6 Max. 22×17×7-3/4	20.0

COARSE POINTING MECHANISM

CASSEGRAINIAN TELESCOPE

IMAGE-MOTION COMPENSATOR

POWER METERS

DETECTORS

RADIATION COOLER

LASER L.O.

LASER XMTR/MODULATOR
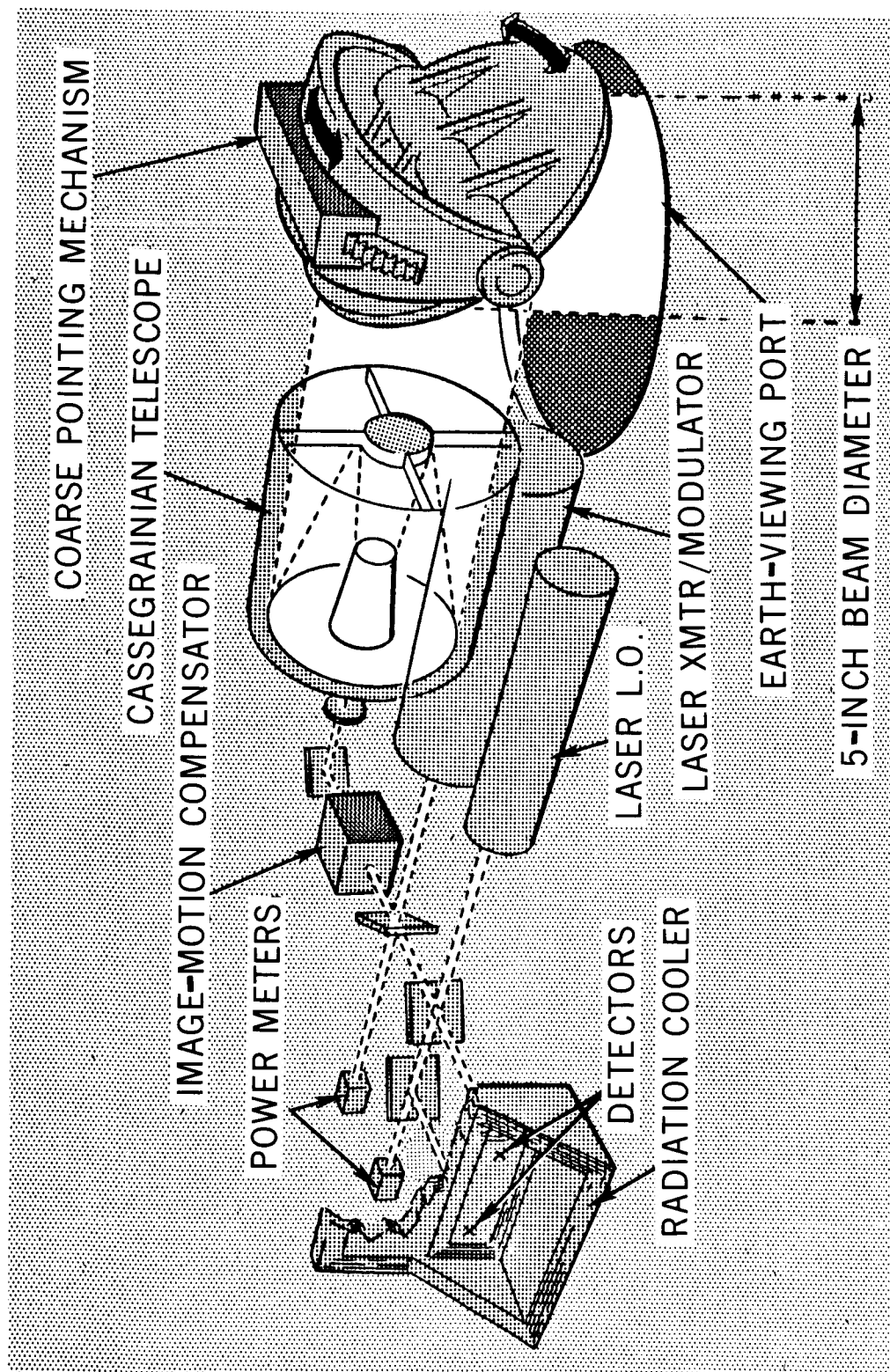
EARTH-VIEWING PORT

5-INCH BEAM DIAMETER

Figure 3. Laser System Conceptual Drawing

9

lubrication using a labyrinth bearing seal has operated for extended periods in space environments. This item is the only mechanically rotating mechanism in the system.

The coarse-pointing mechanism mirror is a lightweight mirror consisting of aluminum or beryllium overcoated with 0.006 ±0.001 inch of Kanegen before optical polishing. Metal mirrors are especially attractive because of their light weight, ease of mounting, high modulus of elasticity, and favorable thermal properties. For 10.6-micron wavelength, the mirror flatness is not seriously degraded in the expected space environment and can be achieved more easily than in the visible wavelengths.

The viewing field of the optical subsystem is governed by several factors: the placement of ATS-G relative to ATS-F, the orbit position of ATS-F, the location of the package on the satellite, and the obscuration by the satellite structure. Viewing, field, satellite location, and packaging concepts will be discussed in detail later.

3.1.2 TELESCOPE

The telescope (optical antenna) required is a 5-inch-aperture system with a 0.2-degree field-of-view. It acts much in the manner of an RF antenna; that is, it focuses the laser output into a high power-density beam during transmission and provides maximum power-gathering area during reception.

The telescope is composed entirely of reflective aluminum or beryllium mirrors. After optical polishing, the mirrors are coated with vacuum-deposited aluminum, either pure or in combination with other materials, to provide high-infrared but low-visible reflectance (Reference 3) (Figure 4). These films, as well as pure aluminum, provide a reflectance as high as 98 percent at 10.6-micron wavelength. Special paints and baffles used in the telescope and telescope housing will reduce scattered light and provide temperature control. Because many of the optical elements and associated mounting structures radiate thermally to deep space, the mirrors themselves will operate at a temperature lower than that of the surrounding satellite. This can be advantageous because cold optical elements emit less background from their own emissions; furthermore, it may be desirable to decouple them thermally from the satellite, thereby reducing the gradient across the optical elements. As mentioned before, gradients are not as serious an optical problem at 10.6 microns as in the visible spectrum.

10

OPTICAL SURFACE COATINGS

Reflectance of Al-SiO filter mirror as a function of wavelength. Layer deposition controlled at 550 mμ

Layer arrangement in Al-SiO-Al-SiO filter mirror

Reflectance of Al-SiO Filter mirror as a function of wavelength. Layer deposition controlled 0.55μ
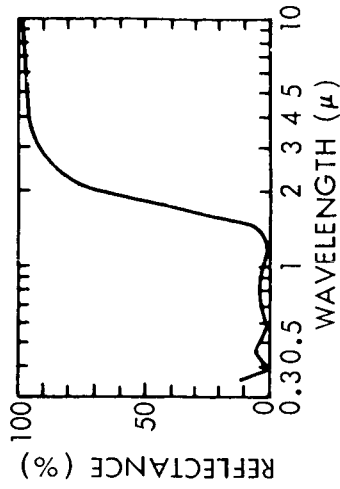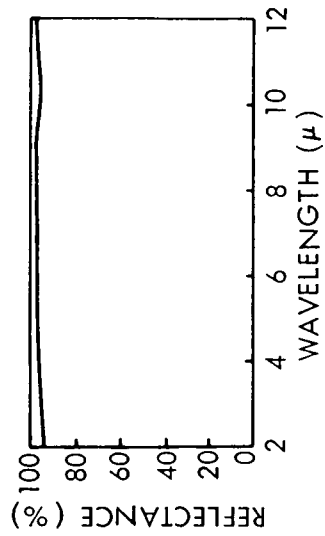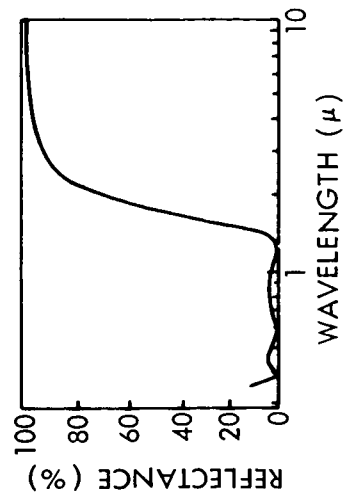
Figure 4. Reflectance Properties of Infrared Coatings

3.1.3 IMAGE MOTION COMPENSATOR

After the telescope collects and focuses the received energy, the energy passes through a negative lens that also acts as a filter. This negative lens collimates the converging telescope rays into a pencil-thin parallel beam which is then directed into the image-motion compensator, or fine-pointing mechanism. Selective mirror coatings and lens filter material eliminate the necessity to shutter the system from direct sunlight. At 10.6 microns, the sun's energy is decreased four orders of magnitude from the value at the peak of its spectrum. When conducting experiments to an earth station, the sun is never in the field-of-view. When conducting experiments to ATS-G from ATS-F, the sun may be within the optical system's 0.2 degree field-of-view only for approximately 1 minute when the sun is in the satellite's orbital plane, which happens twice per year.

The image motion compensator corrects instabilities in satellite pointing. The satellite will be earth-oriented and stabilized by a 3-axis inertial-wheel control system to a specified accuracy of ±0.1 degree, with a jitter rate of 0.0003 degree per second. The required pointing accuracy of the optical system, on the other hand, is approximately ±0.003 degree, representing a dynamic control-range requirement of only 36:1. Satellite operational fine-guidance systems operate at dynamic range levels as high as 200:1 (200 resolution elements). To implement fine control of optical beams over a relatively narrow field-of-view, new operational techniques are being developed to supplement older, well proven techniques, such as the galvanometer movement that can steer optical beams very precisely without causing large bearing-supported components to be moved.

One technique the GSFC Optical Systems Branch employs for optical beam steering is based on small piezoelectric bender bimorphs as the active deflection elements (Reference 4). A simplified diagram of the optical beam-steerer configuration is shown in Figure 5. By moving one mirror in a direction orthogonal to the movement of the other mirror, an infinite number of beam directions may be obtained to within the resolution of the system. For initial beam acquisition, the coarse beam pointing mechanism is commanded to point to either the ground station or ATS-G. The ground station or ATS-G laser transmitter beam by-passes its five-inch optical system and is pointed at ATS-F within ±0.1 degree. By bypassing the transmitter beam around the five-inch optical system, a diffraction-limited beam with an angular divergence of ±0.11 degree is produced. This beamwidth is greater than the angular instability of ATS-F. Therefore, the ATS-F satellite is illuminated by the broad beam. A command is then sent to ATS-F, via the telemetry link, to start the search-scan operation. Once ATS-F has achieved "lock-on", the ATS-F transmitter is turned on and it serves as a beacon for lock-on by the receiver at the ground station or on ATS-G. The search-scan operations are performed by the application of appropriate voltages to the piezoelectric bender bimorphs.

12

The present system (Figure 6) provides a performance exceeding the requirements for the laser optical communication experiment.

3.2 LASER SUBSYSTEM

Two lasers will be used in the spacecraft package: a 50-mw local oscillator (LO) weighing 2 pounds and occupying a 2- by 2- by 8-inch volume, and a

MIRROR
0.5" DIA.

PIEZOELECTRIC
BENDER BIMORPH

LASER BEAM

MIRROR
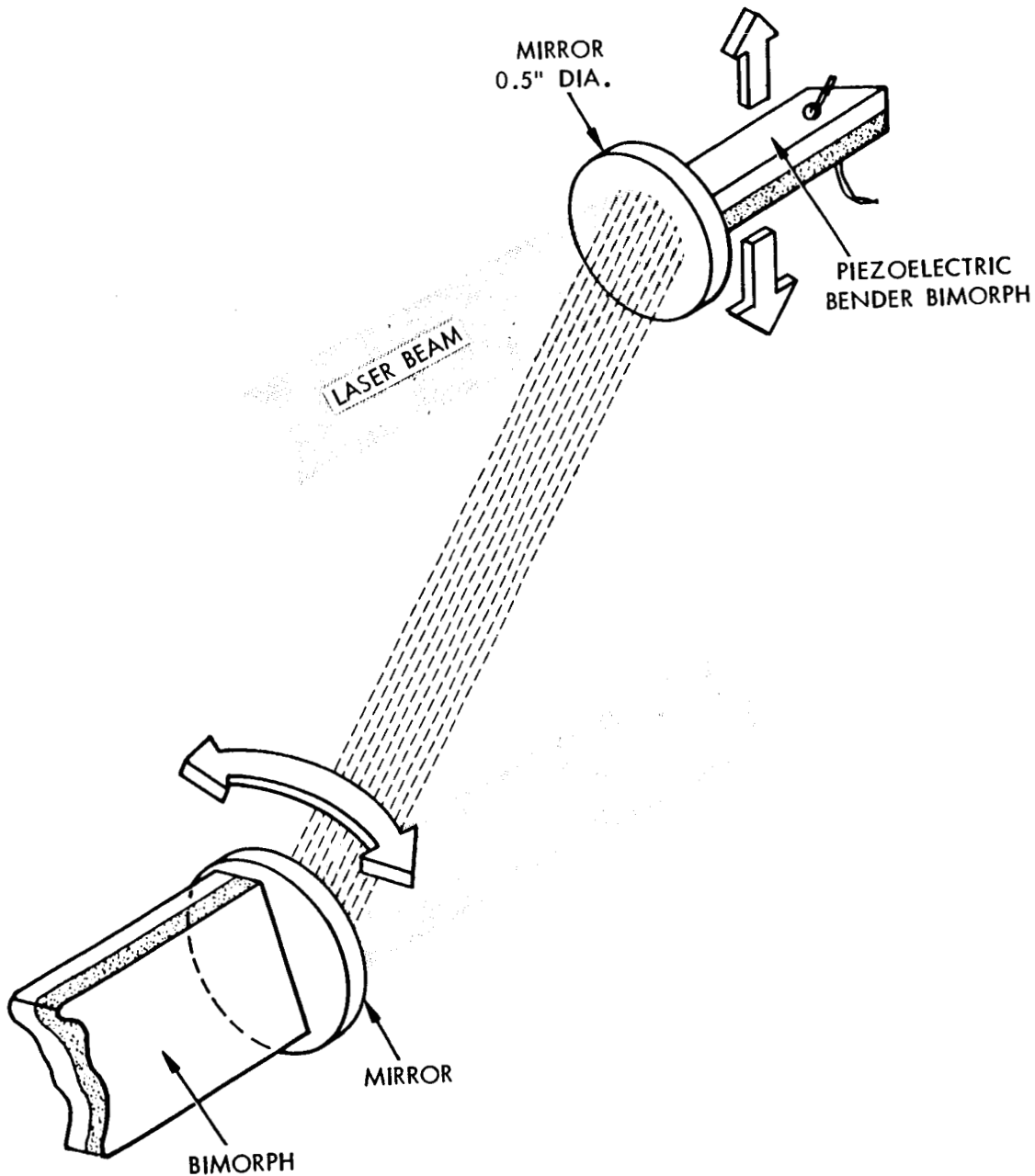
BIMORPH

Figure 5. Image-Motion Compensator Beam Steerer Configuration
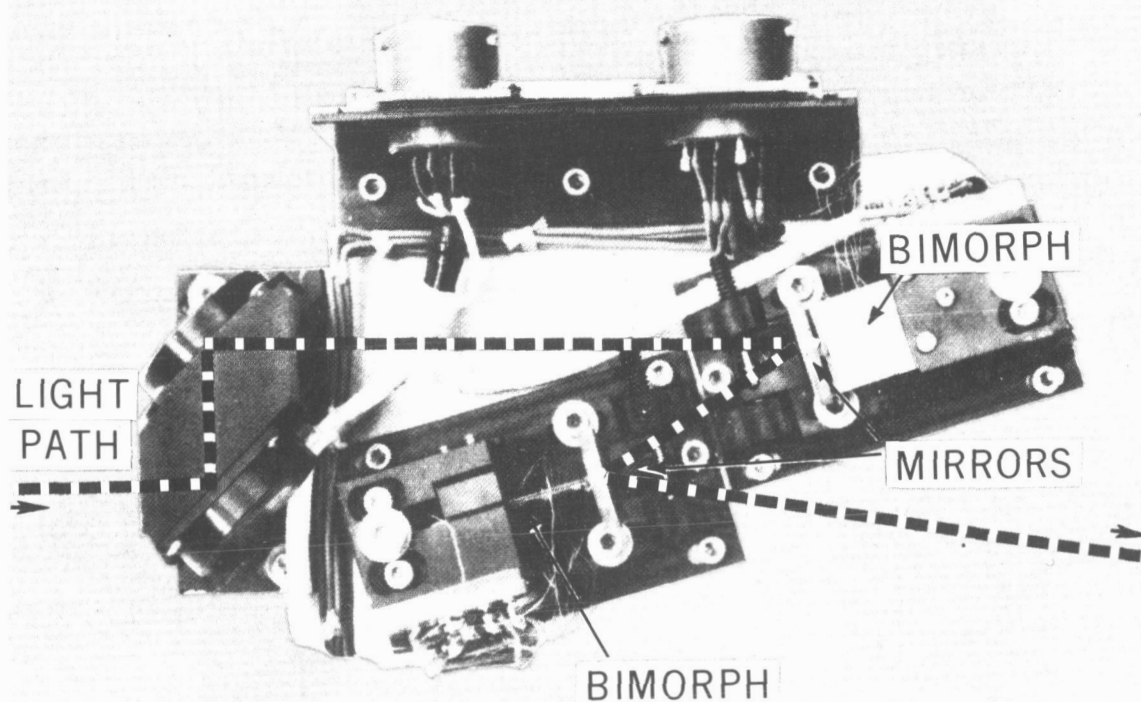
Figure 6. Image-Motion Compensator Using Bender Bimorph

transmitter slightly larger. The transmitter, generating 400 mw of carrier power, has a modulator within the resonator cavity, providing FM with a 15-MHz modulator bandwidth.

Figure 7 is a functional diagram of the laser and laser control electronics.

The theory of CO_2 lasers, stressing only those aspects pertinent to their operation as signal generators, will be discussed in the following paragraphs.

Amplification is achieved at select frequencies in the 28-tHz band by ionizing CO_2 gas in a plasma tube at a gas partial pressure of 1 torr; the amplification gain is about 2 db per meter. Figure 8 shows a spectral plot of the amplifying bands.

Regenerative amplification results from placing the plasma tube in an infrared resonator. The resonator cavities commonly used are formed by two concave mirrors optically aligned to face each other (Figure 9). Radiation is coupled out of the cavity by adjusting the partial transmission through one of the resonator mirrors. The simplest and most common standing-wave patterns

14
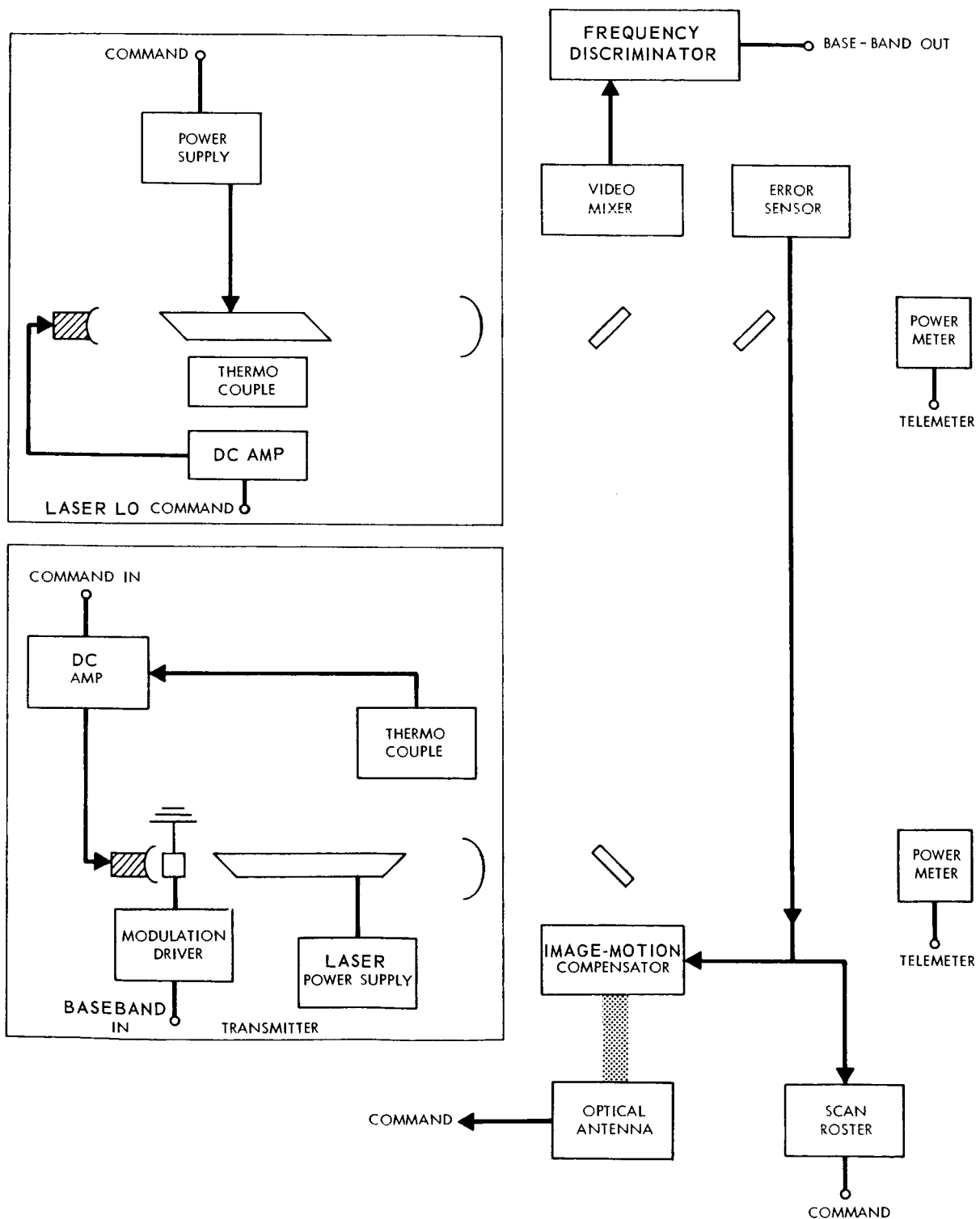
Figure 7. Functional Diagram of Laser Control and Electronics
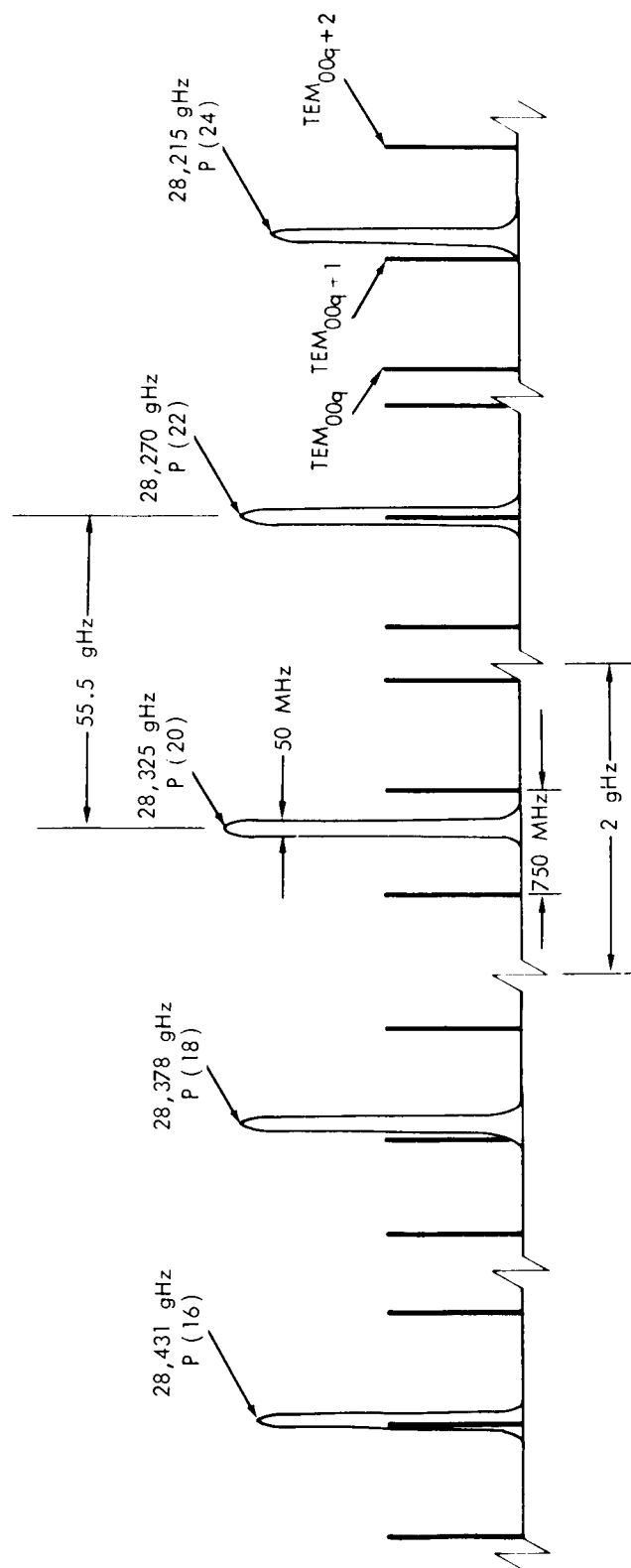
Figure 8. Spectral Plot of the Amplifying Bands
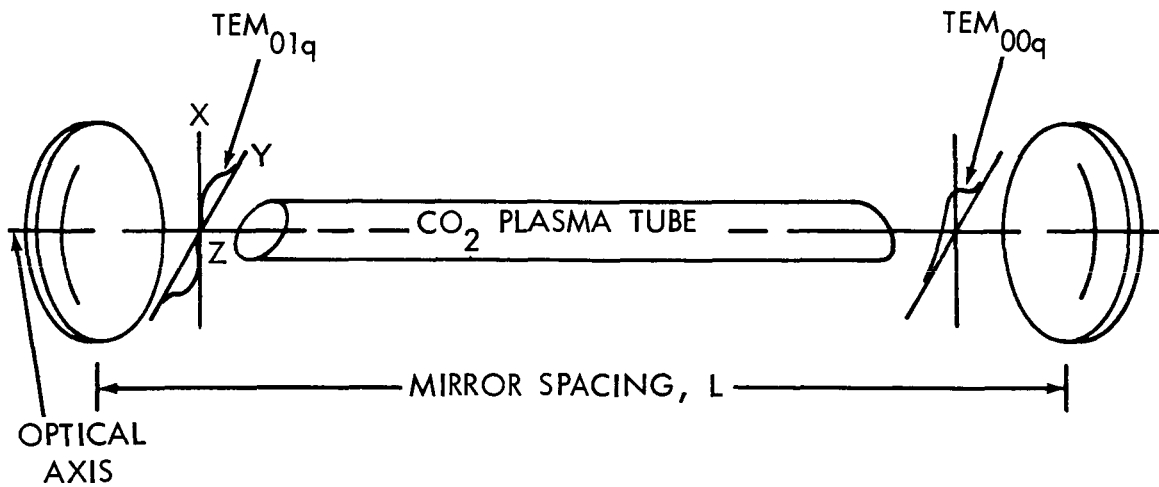
(In practice the mirrors are rigidly held to close tolerance by low thermal expansion material to minimize resonator frequency drift. Graph shows electric field intensity of the TEM_{o1q} mode and TEM_{ooq} modes along the X-axis.)

have transverse electric and magnetic fields, designated by TEM_{nmq}. The subscripts indicate the number of nulls of the standing-wave pattern in the X, Y, and Z axes, respectively, just as in the analogous microwave cavities (Figure 9).

The following boundary conditions are required to form a stable, high Q resonance cavity at a particular frequency: the mirror spacing must be less than the sum of the mirror radii, and the mirror spacing must be an integral number of half waves. For the TEM_{ooq} mode used in the oscillators, the resonance frequency is determined by

$$q\pi = \beta L, \tag{1}$$

where L is the mirror spacing, q is a large integer, and β has the conventional meaning, $2\pi/\lambda$. The spacing between adjacent modes is obtained from Equation 1 by

$$(q + 1) \pi - q\pi = (\beta + \Delta\beta) L - \beta L, \tag{2}$$

which gives

$$\Delta f = \frac{c}{2L} \qquad \text{(3)}$$

For the experimental 20-cm mirror spacing used in the spacecraft, LO, we obtain a Δf = 750 MHz from Equation 3. Figure 8 shows the cavity resonance superimposed on the plot of amplifying bands.

It is quite possible for resonance mode frequencies to fall into more than one amplifying band. In Figure 8, for example, resonance conditions occur under both the P(16) and P(22) CO_2 spectral lines. Under such conditions, simultaneous oscillation could occur in both molecular resonance lines at frequencies separated by 55.5 gHz or more. Experiments have shown, however, that only the highest active Q mode will oscillate (Reference 5). This is important to the experiment, because we must ensure that the satellite LO oscillates in one band only. The transmitter carrier and LO must be within the same spectral line, which, as shown in Figure 8, is only 50 MHz wide. To maintain system reliability, the IF will be kept at 20 MHz and transmitter RF spectrum less than 30 MHz, thus ensuring that oscillation occurs well within the 3-db points of the amplifier line.

An open servoloop makes it possible to maintain the LO frequency within 15±1 MHz of line center on one side and the transmitter carrier within 5±1 MHz of line center on the other side.

The assumed temperature stability within the flight package is 20°C ±10°C. Figure 10 shows a CO_2 laser with a Cervit mirror mount designed under Honeywell, Inc., contract NAS8-20645, for low thermal expansion. The expansion coefficient of Cervit at 20°C can be made as low as 10^{-7} deg^{-1}. Using Equation 1, the frequency variation as a function of mirror spacing is

$$\frac{\Delta f}{f} = \frac{\Delta L}{L}. \qquad \text{(4)}$$

From the definition of thermal-expansion coefficient, α, we have

$$\alpha \Delta t L = \Delta L. \qquad \text{(5)}$$
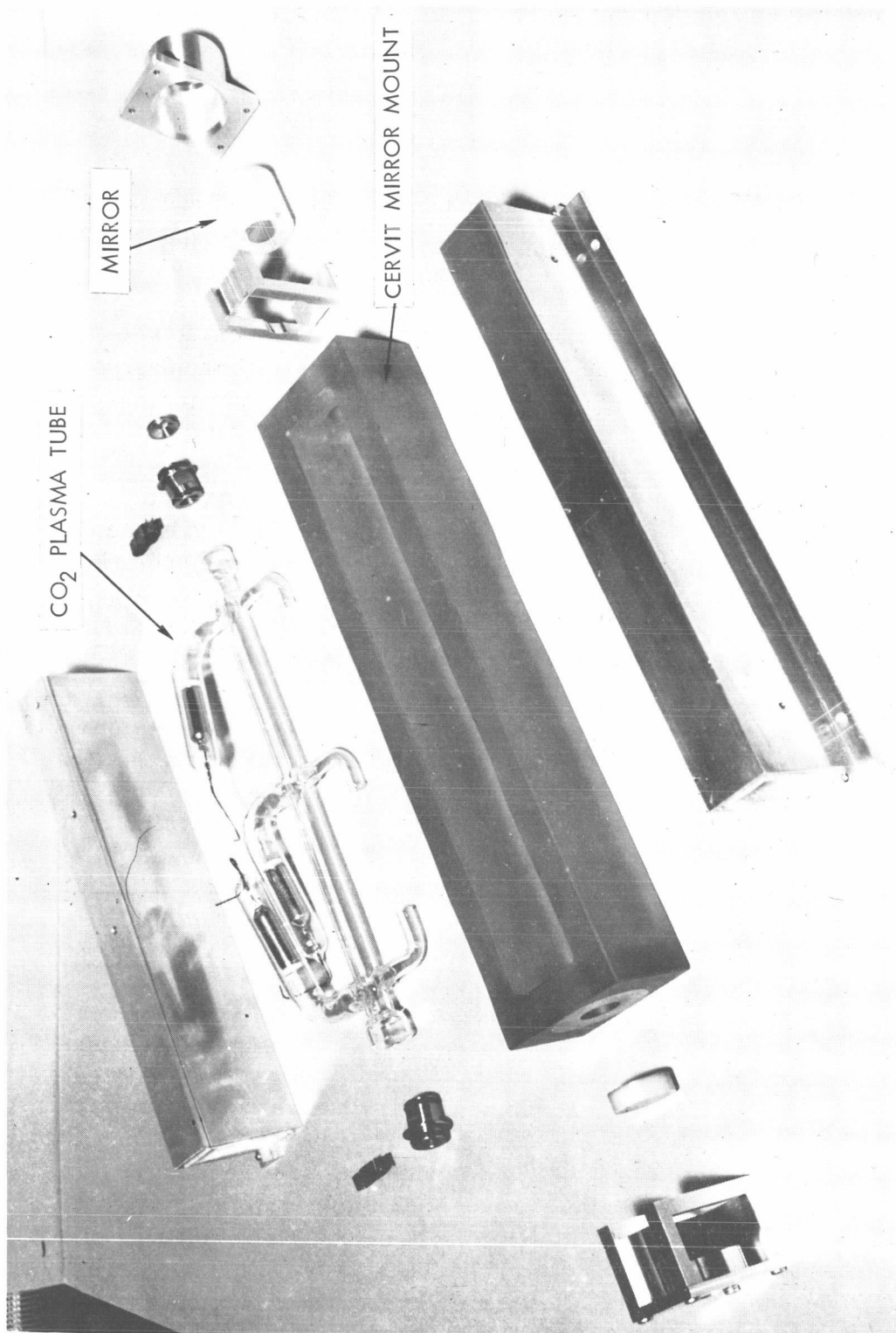
MIRROR

CERVIT MIRROR MOUNT

CO2 PLASMA TUBE

Figure 10. Dismantled CO_2 Laser
(Photo courtesy of Honeywell, Inc.)

Combining these equations, the following laser-frequency versus mirror-housing temperature relationship results:

$$\Delta f = f \Delta t \alpha. \tag{6}$$

For a 20°C temperature swing, Equation 6 predicts a 54-MHz laser frequency change when using mirror spacers with a 10^{-7} deg^{-1} thermal-expansion coefficient.

Lasers have been developed with tuning capability sufficient to allow servo-control providing the required 1-MHz accuracy. To illustrate the degree of control over laser frequency, we quote from the instruction manual for an operational laser used at GSFC (Reference 6):

> The non-output mirror used with the laser is mounted on a piezo-electric stack — The transducer allows controlled physical movement of the non-transmitting laser mirror which, in turn, allows the operating frequency of the laser to be controlled and adjusted. The power supply has a coarse and fine control of the output voltage, allowing the laser frequency to be controlled to within about 50 kHz manually.

> In normal operation, the power supply voltage should be set to about 300 volts to read on the front meter and then adjusted to obtain the desired output frequency or wavelength. The sensitivity of the power supply-transducer system for this laser is about 1 MHz per volt. That is, the laser output frequency is changed by 1 MHz for every volt change in supply voltage. Since the Doppler linewidth of the CO_2 laser transition is about 50 MHz, a 25-volt change in the transducer supply voltage may be all that is required to tune across the gain curve for a particular wavelength.

Tabe 2 lists general characteristics of typical CO_2 laser oscillators at the present state of development.

Modulation is most efficiently achieved by varying the resonant frequency of the oscillator resonator. The ATS laser communications experiment will use tried and proven FM techniques (Reference 7). A single crystal of GaAs, approximately 1 inch long, is placed in the resonator, and a 122-volt rms signal is imposed across the crystal transverse to the laser beam within our power budget. The power is consumed primarily in the matching resistor outside the laser resonator, rather than dissipated in the modulator crystal. Thus, laser frequency

20

drift arising from resonator temperature change will not be caused by the modulator. The power consumption in the modulator drive circuitry is

$$P = \frac{1}{6} C\omega V, \tag{7}$$

·where

C is the crystal capacitance, 6 pf,

ω is the modulator bandwidth, and

V is the rms drive voltage.

Thus, 0.7 watt of drive power will be required for 30 MHz of RF bandwidth. Options are open to trade among signal-to-noise, modulator power, bandwidth, and modulation index.

3.3 DETECTOR SUBSYSTEM

3.3.1 SIGNAL INFORMATION DETECTOR

The optical subsystem directs the incoming infrared signal information to the signal information detector. Coherent heterodyne detection is proposed for this experiment because it is superior by six orders of magnitude to direct envelope detection in sensitivity and ability to discriminate against background. Heterodyne detection involves the coherent mixing of the incoming laser signal with the local oscillator at the detector, which has a square law response. The emergence of coherent laser technology has now made possible the performance of this function, analogous to radio-frequency techniques. The ultimate sensitivity limit for heterodyne detection, termed the quantum limit, is $2h\nu\Delta f$ or, nominally, 10^{-20} watts per cycle of bandwidth. Recent measurements by Arams (Reference 8), Teich (Reference 9), and Mocker (Reference 10) have shown that sensitivities within a factor of 2 of the quantum limit are attainable (Figure 11).

The detector used will be a sensitive wideband mercury cadmium telluride detector of 10.6-micron energy, which can be operated at temperatures well above that of liquid nitrogen (77°K). This capability makes possible the use of

Table 2
Laser Oscillator Characteristics

Characteristic	Datum	Author	Source
Short-term frequency stability (10^{-3} sec)	3 kHz	R. E. Reynolds, Sylvania; Hans Mocker, Honeywell, Inc.; Charles Freed, MIT, Lincoln Lab.	NAS-510309 NAS-510309 1968 International Quantum Electronics Conference; Miami, Florida
Long-term frequency stability (Hours)	1 MHz		See text
IF receiver tracking bandwidth	2500 Hz	T. E. McGunigal, GSFC	Stable CO_2 Laser. Quarterly Progress Report ART/SRT. Research and Advanced Technological Developmental Activities. Goddard Space Flight Center, vol. 3, No. 3, p. 9, March 1968
ARC receiver with tracking laser LO bandwidth	500 Hz	F. E. Goodwin Hughes Aircraft; T. A. Nussmeier, Hughes Aircraft; Hans Mocker, Honeywell, Inc.	Private communication Private communication NAS-8-30645
Oscillator life time	More than 1000 hours	Peter Clark, Hughes Aircraft; W. J. Witteman, Philips	AF33(615)-5253 Applied Physics Letters, Dec., 1967
Oscillator efficiency	8%	F. E. Goodwin, Hughes Aircraft; T. A. Nussmeier, Hughes Aircraft	AF33(615)-5253 AF33(615)-5253
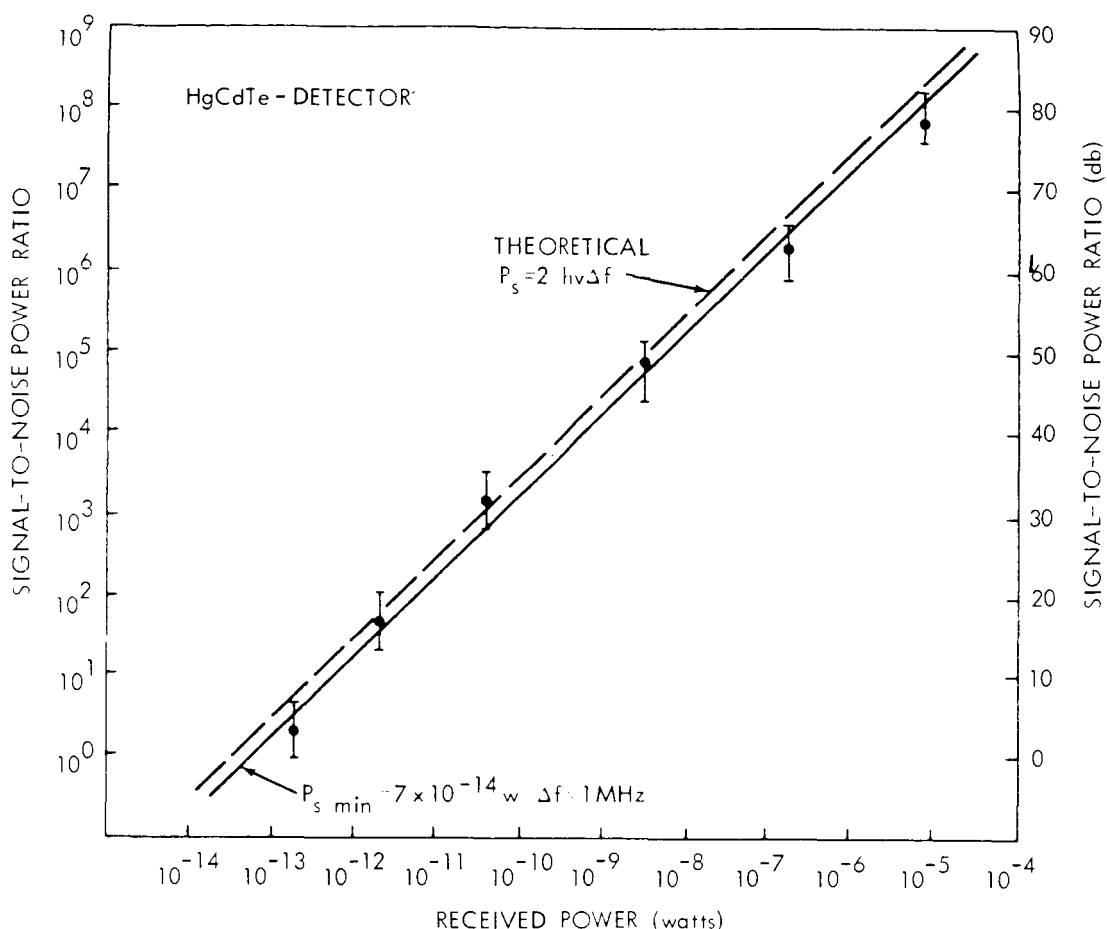
Figure 11. Far-Infrared Mixer Sensitivity Measurements Made on a HgCdTe Element (Noise Bandwidth of IF System, 1 MHz.) (From Reference 10)

high-performance 10.6-micron detectors in space applications. Previously available detectors with comparable performance parameters required liquid-helium operating temperatures (4.2°K) or, at the very highest, temperatures in the vicinity of 20°K. The possibility of obtaining satisfactory performance at increased temperatures, up to 100°K, allows the use of radiative coolers that required no power from the satellite's power supply, and have very low weight and an extremely long operating lifetime. The effect of operating temperature on detectivity of a HgCdTe IR mixer appears in Figure 12, which shows that a detector having a D* of 4.5×10^{10} cm Hz$^{1/2}$/watt at 77°K will have a D* of nominally 3.5×10^{10} cm Hz$^{1/2}$/watt at 100°K, and 5.0×10^{9} cm Hz$^{1/2}$/watt at
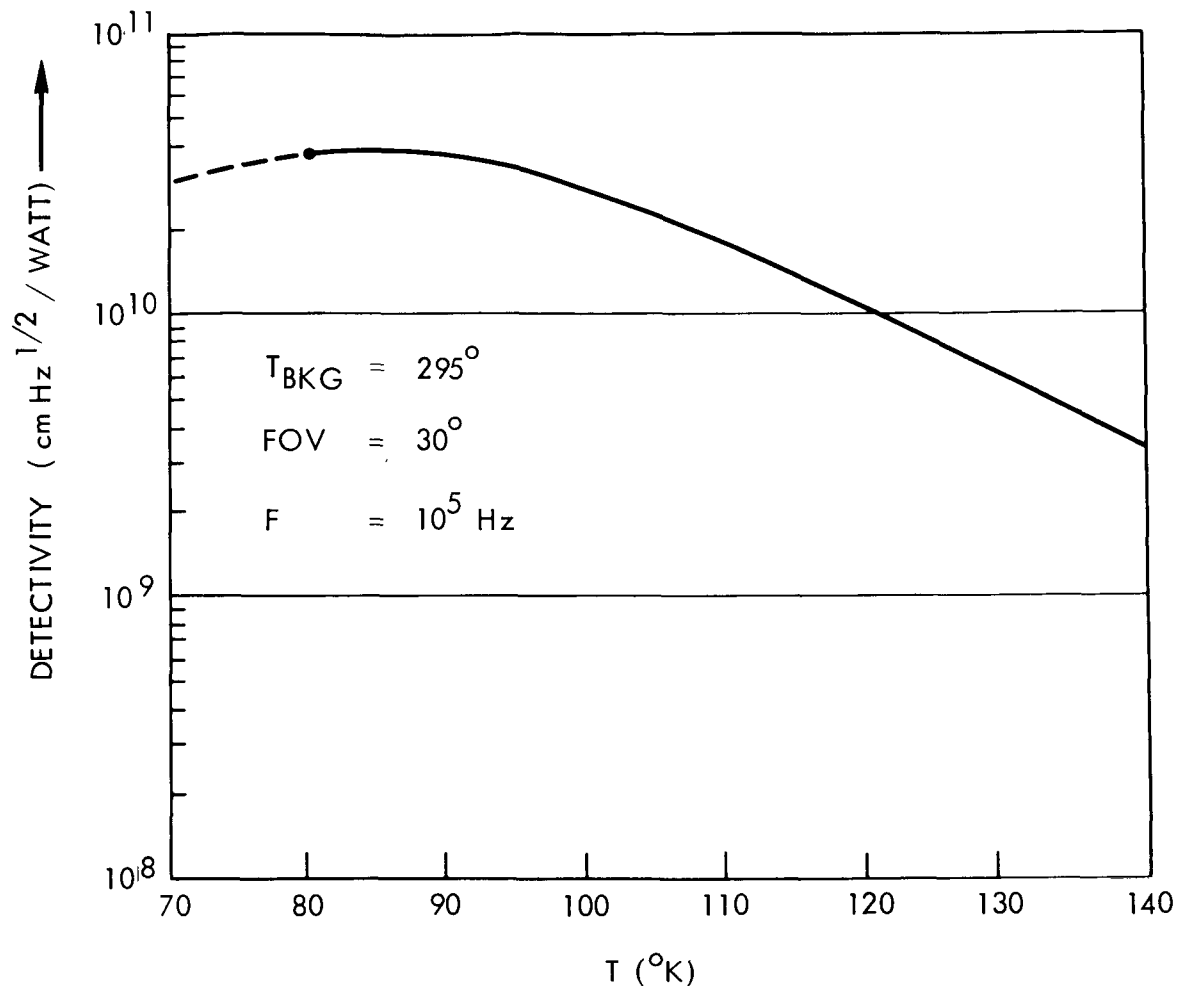
Figure 12. The Effect of Operating Temperature on Detectivity of an IR Mixer
(From Reference 10)

130°K. Mocker (Reference 10) has reported the achievement of a frequency response exceeding 50 MHz at a temperature of 77°K, requiring only 2 mw of local oscillator power, to approach quantum noise-limited operation with this material.

The output of the video mixer is supplied to a broadband preamplifier having a bandpass from 5 MHz to 35 MHz. The preamplifier output connects to a coherent demodulator that may, for instance, feed the intelligence signal to the RF cross-strap.

3.3.2 FINE BEAM-POINTING ERROR SENSOR

The fine beam-pointing error sensor provides the servo signals necessary to operate the image-motion compensator that controls the direction of transmitted

and received rays. Sensor operation can be divided into two modes: acquisition and tracking. The acquisition mode starts when the image-motion compensator initiates a scan program; it terminates when the error sensor registers acquisition of received radiation and sends a command to the scan program to halt the scanning operation. The tracking mode starts with the acquisition of a signal. After acquisition has been registered, the image of the incoming laser beam is automatically centered on the sensor. Subsequent drifts in the image position result in azimuth and elevation error voltages that cause the image-motion compensator to recenter the image.

As in the signal information detector, heterodyne detection will be used for maximum sensitivity. HgCdTe detectors will be used because of their excellent performance at temperatures near 100°K. The beam-pointing error sensor consists of four detectors (Figures 13 and 14). Each detector is followed by an identical sequence of preamplifier, filter, and RF detector. The optical system that directs the received laser energy to the signal detector also supplies the signal to the error sensor. Since it is presumed that the incoming beam direction is uncertain over a range of 720 arc-seconds (±0.1 degree), the diffraction-limited spot size on the error sensor detector is designed to be 40 arc-seconds, producing 18 resolution elements across the focal plane. Therefore, if the detector dimensions are matched to the resolution element, the exact spot location could be determined if an array of 18 by 18 detector elements were placed at the focal plane. To avoid the complexity of such a system and the associated logic circuitry, a 2 by 2 array is employed in conjunction with a scanning system that uses the image-motion compensator.

The scanning programmer causes the image-motion compensator to begin a rectangular raster scan covering the 0.2-degree field. The dwelling time at each position is in accordance with the tracking bandwidth. The dwelling time is also long enough to permit acquisition when the beam strikes one detector element. The experiment design results in typical acquisition times of much less than 1 minute. After acquisition, a scan stop command is sent to the scanning programmer, which halts and locks the scan of the image-motion compensator to center the image on the sensor. Henceforth, imbalances in the power reaching the four detectors produce azimuth and elevation error voltages that direct the image-motion compensator to reposition the image.

3.4 EXPERIMENT LOCATION AND PACKAGING

3.4.1 CHOICE OF EQUIPMENT MODULE

The ATS-F and -G configuration provides two equipment modules for packaging experiments and satellite housekeeping subsystem components. In the orbital configuration, the earth-viewing module (EVM) is located below the 30-foot
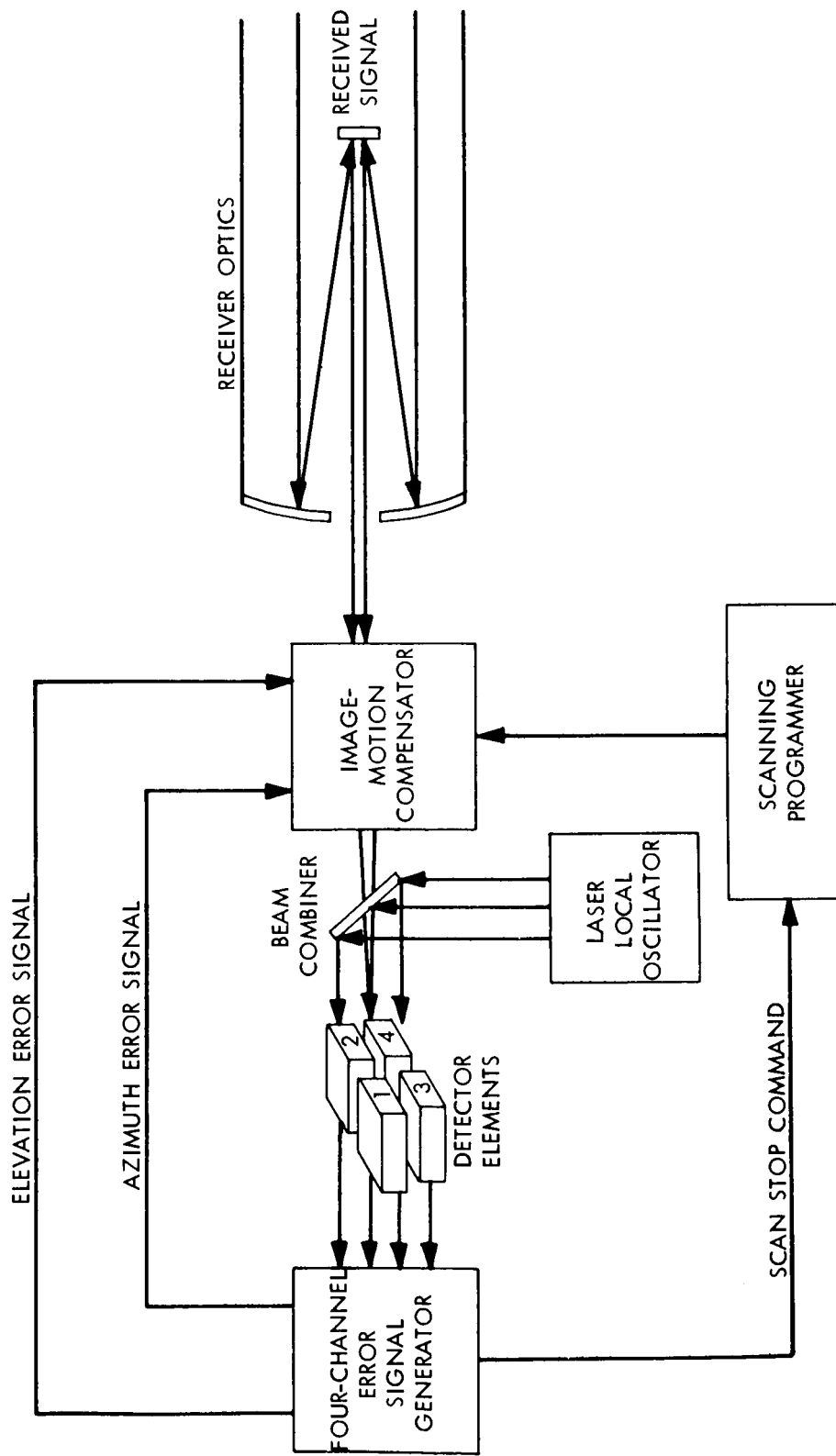
Figure 13. Block Diagram of Fine Beam-Pointing Control

RECEIVER OPTICS

RECEIVED SIGNAL

IMAGE-MOTION COMPENSATOR

SCANNING PROGRAMMER

BEAM COMBINER

LASER LOCAL OSCILLATOR

ELEVATION ERROR SIGNAL

AZIMUTH ERROR SIGNAL

DETECTOR ELEMENTS

SCAN STOP COMMAND

FOUR-CHANNEL ERROR SIGNAL GENERATOR
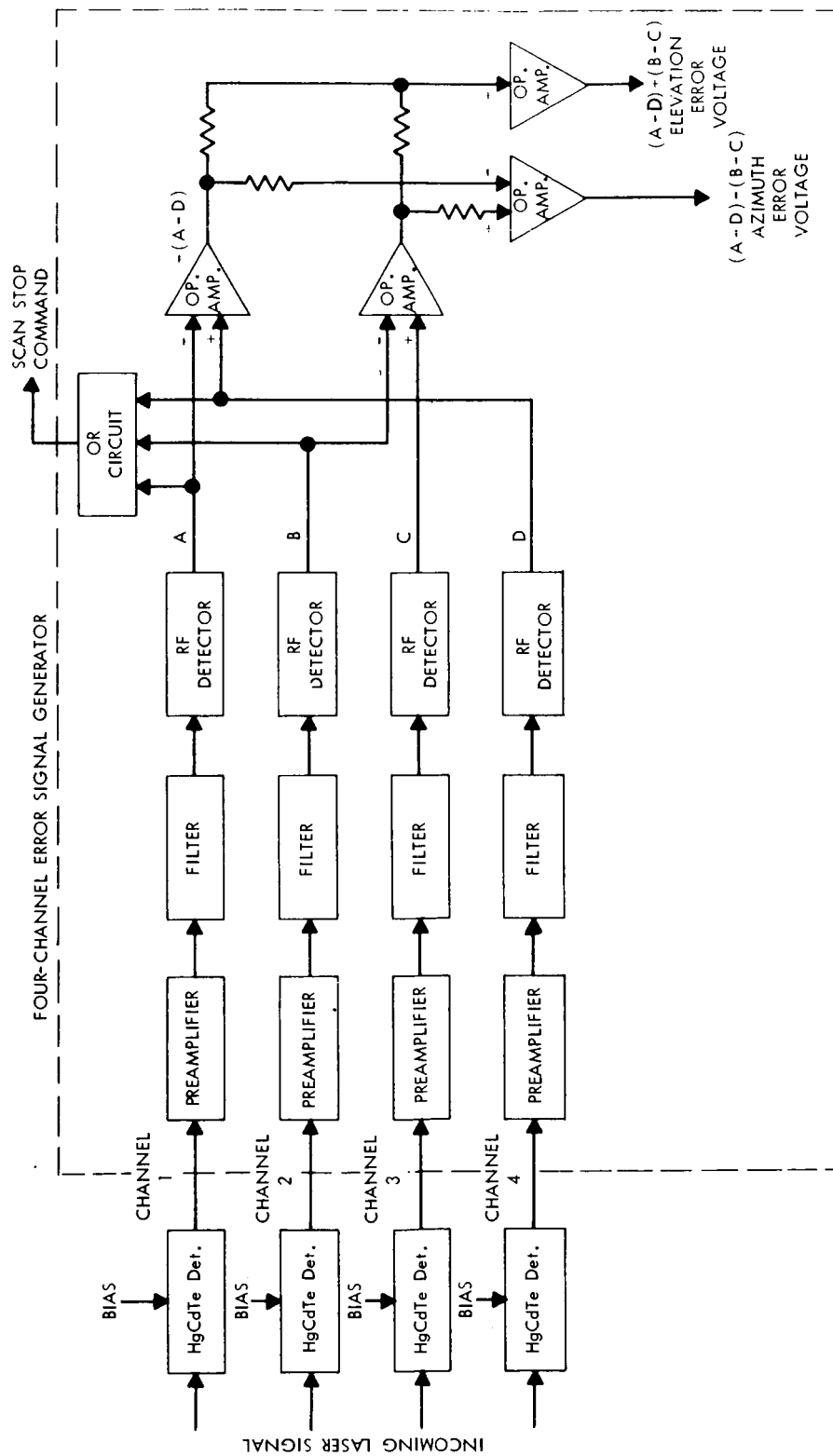
26

Figure 14. Beam Compensator Error-Sensing Circuit

27

parabolic reflector and provides clear unobstructed fields-of-view to earth and to any point in the geostationary orbit. The aft module located behind the reflector provides a very limited viewing area to the earth, but is ideally suited for deep-space viewing experiments.

Thus, the EVM seems to be the obvious location for the laser because it requires a field-of-view to earth for ground checkout and to the orbit path for communication with other ATS satellites. However, the competition for earth-viewing area is keen among the primary experiments (interferometer, attitude-control subsystem earth sensor, communications subsystem standard gain horns) and the telemetry, tracking, and control (TT&C) subsystem. Adding one more aperture to the earth-viewing face of the EVM would further restrict the selection of experiments that must view earth. Also, the thermal-control requirements of the laser experiment are best met by providing a large north/south-facing area. However, the optimum north/south-facing, heat-rejection areas on the EVM are also in high demand by the primary experiment communications transponders. Finally, for structural efficiency and minimization of overall mission weight, the EVM should contain only those experiments absolutely necessary to accomplish the mission.

Consequently, overall ATS mission performance can be improved if experiments are located in the aft module, where thermal-control area and packaging volume are more abundant and where the addition of items incurs the least structural weight penalty. The vibration qualification-test levels will be lower in the aft module than in the EVM, where high transmissibilities to launch environments occur. This is also significant to the laser experiment. Therefore, the aft module appears to be the most reasonable location for integrating the laser experiment with the ATS-F and -G.

3.4.2 VIEWING-FIELD CONSIDERATIONS

Placing the laser experiment in the aft module introduces some field-of-view constraints: namely, the projected beam must clear the earth-viewing module, the K-frame struts, and the reflector retention framework. Obscuration by the K-frame members can be eliminated by selecting an equipment bay having a proper circumferential orientation with respect to the K frame. In addition, north- or south-facing bays are necessary for optimum thermal control.

To justify selection of an equipment bay, a brief discussion of the 30-foot parabolic reflector constraints on the spacecraft is warranted. The K-frame strut configuration has been selected to allow the antenna to be folded around the struts in the satellite launch configuration with a minimum number of folded sectors (12). Twelve chain-driven screw-jack actuators activate a truss structure that deploys the antenna. The solar-paddle support and deployment arms

28

are integral with this deployment system. The 21-inch screw-jack actuators are radially spaced around the aft module. This stowage configuration introduces the following constraints:
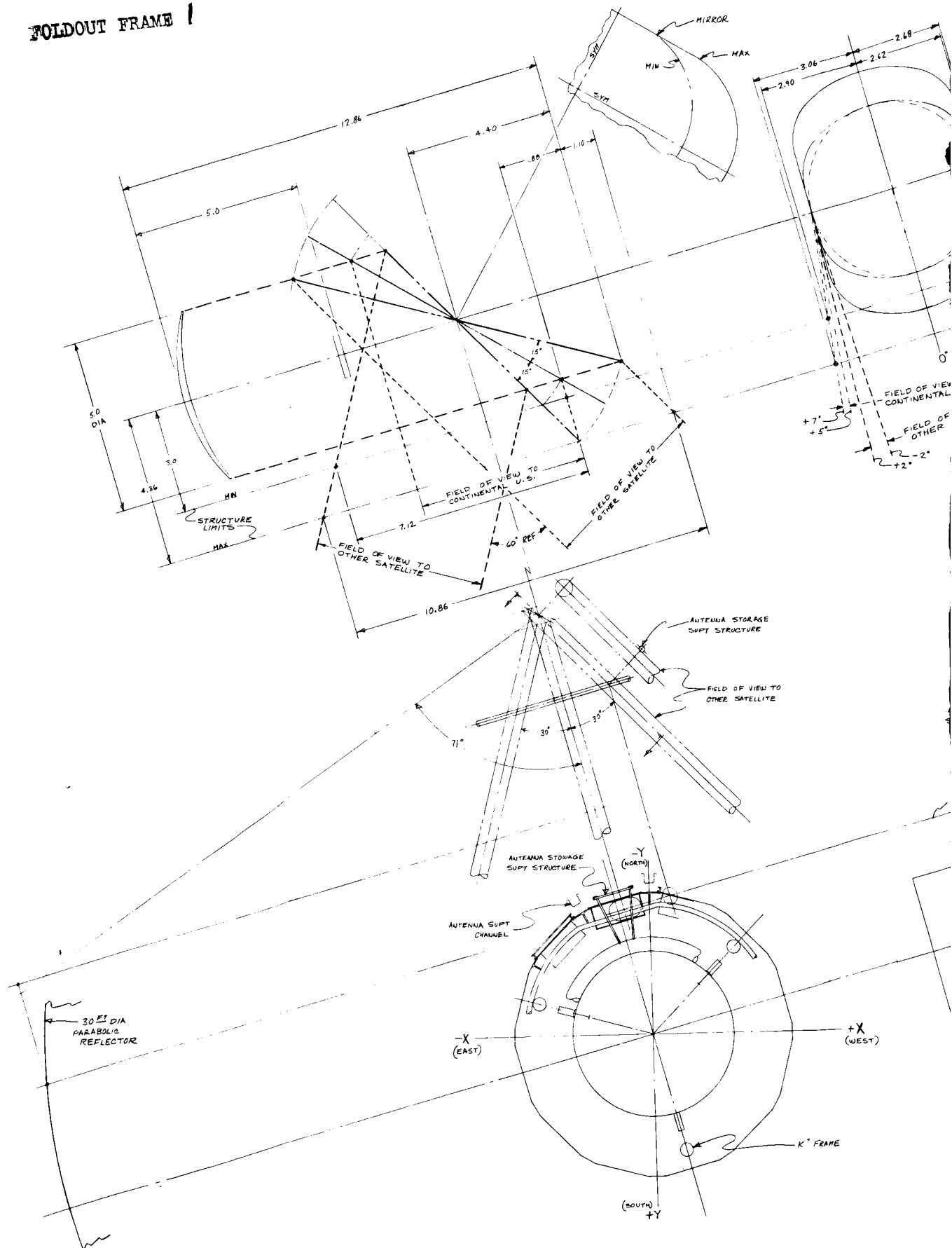
- The aft-module heat-rejection surface is segmented into 12 areas that lead to 12 equipment bays whose maximum heat rejection area is 17 by 22 inches per bay.

- The solar paddles must be located along the north-south axis; therefore, their screw-jack actuators must also be on the north-south axis. This orients the entire deployment system so that no resulting equipment bay is truly north or south.

- The K-frame struts, which must be located within the folded antenna, have to be displaced 7.5 degrees from the screw jacks, thereby intersecting the aft module in the center of three equipment bays.

- To support the petals in the stowed position, an additional support structure is built onto the K-frame struts. A spider or framework of aluminum members is provided at the earth-viewing end of the configuration. These pick up the open-end hinge lines, giving the folded cylinder stiffness. At the aft module, a circular ring supports padded clevises that pick up the interior hinge lines.

A reference to Figure 15 will show the influence of these constraints on the installation of the experiment. The four north and south equipment bays are optimal for thermal control, since the radiation cooler must view cold space. To cover the entire continental United States while the satellite yaw axis is pointing to the subsatellite point, it may be necessary to introduce into the present conceptual structure configuration minor changes such as the local flattening shown on the antenna support ring.

For a trisatellite communications link, pointing to 30 degrees east or 30 degrees west is required; for satellites closer together, this angle would increase. If the northeast or northwest bay were chosen, a view toward ATS-G in the respective east or west direction would never be blocked by the spacecraft structure.

Figure 15 shows the EVM structure does not interfere with pointing, provided the K-frame strut members are oriented as shown. Locating one truss member over either south-facing bay will keep the other two members well out of the orbital viewing plane. This is a reasonable location, because no other mission or spacecraft design requirement constrains K-frame orientation.

MIRROR

MAX

MIN

SYM

12.86

4.40

.88

1.10

3.06

2.62

2.90

2.68

5.0

5.0 DIA

3.0

4.36

MIN

STRUCTURE LIMITS

MAX

15°

15°

FIELD OF VIEW TO CONTINENTAL U.S.

FIELD OF VIEW TO OTHER SATELLITE

FIELD OF VIEW TO OTHER SATELLITE

7.12

60° REF

10.86

FIELD OF VIEW CONTINENTAL

FIELD OF OTHER

+7°

+5°

+2°

+2° - 2°

0°

ANTENNA STORAGE SUPT STRUCTURE

FIELD OF VIEW TO OTHER SATELLITE

30°

30°

71°

ANTENNA STOWAGE SUPT STRUCTURE

-Y (NORTH)

ANTENNA SUPT CHANNEL

30 FT DIA PARABOLIC REFLECTOR

-X (EAST)

+X (WEST)

K' FRAME

(SOUTH) +Y

TO
U.S.

VIEW TO
SATELLITES

PARABOLIC
REFLECTOR

28 TH$_2$ COMMUNICATION LASER EXPERIMENT

FIELD OF VIEW TO
CONTINENTAL U.S.
(5.0° DIA BEAM)

+7°

ANTENNA STOWAGE
SUPT STRUCTURE

+6°

0°

AFT EQUIP MODULE (A.E.M.)

ANTENNA
STORAGE
SUPT
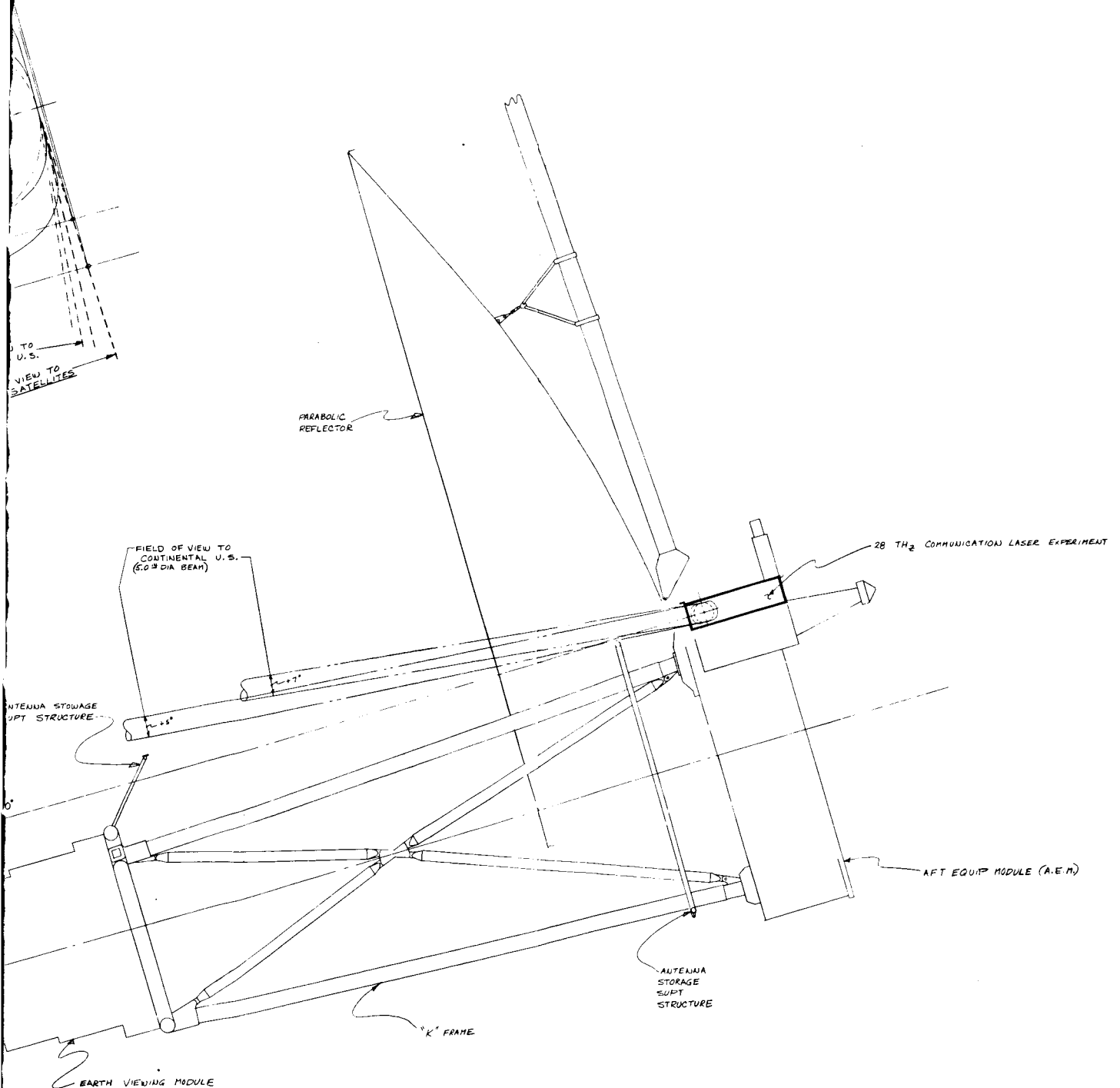STRUCTURE

"K" FRAME

EARTH VIEWING MODULE

Figure 15. Field-of-View and Equipment Location

31

For on-axis pointing to an earth station, or for the capability of pointing in any direction along the equatorial plane, the optics field-of-view is still restricted by the abovementioned antenna petal support ring at the base of the K frame.

Two solutions are available to maintain a clear field-of-view:

- The support ring may be relocated towards the EVM. This is a minor change and considered justifiable until antenna-vibration surveys point out the optimum locations for antenna petal support.

- The support ring may be reconfigured to keep clear of the experiment optics.

The field-of-view requirements also constrain the package dimensions. For a 5-inch laser beam, a 7- by 5-inch elliptical mirror is necessary to reflect the beam 90 degrees towards earth. When reflecting the beam eastward, 5/Sin 60° = 5.8 inches is the required mirror length, but when reflecting westward, 5/Cos 60° = 10 inches of mirror length is required. The resulting mirror shape, including the north-south gimbaling requirements, appears in the drawing. This mirror size, based on a 30-degree east-west scan, has been used in proportioning the equipment module and, with the previously mentioned antenna constraints, fixes the maximum dimensions of the packaging volume at 17 by 22 by 7.75 inches.

If the direction of ATS-G relative to ATS-F is known beforehand, two alternate design approaches may be considered (in either case, the mirror need not be longer than 7 inches):

- If ATS-G is to be located in a trisatellite position, then 30 degrees pointing capability in one direction is required, and the package width can be reduced from 17 to 15 inches.

- If a greater pointing capability in one direction is desired (for instance, if ATS-G were to be closer to ATS-F), then the package would remain 17 inches wide, but pointing 50 degrees in either the east or west direction would be possible.

The package dimensions can be further reduced by considering a design with secondary mirror obscuration. Examination will show that the secondary obscuration (τ_s) depends on the beam-pointing angle:

$$\tau_s = \frac{\pi D^2 \sin \theta}{4} ,$$

where

$$D = \text{diameter of secondary mirror}$$
$$\theta = \text{beam pointing angle from Z-axis.}$$

For a 1.5-inch secondary obscuration, τ_s = 0.3 db. If the geometry is more convenient, such a small degradation would render a design with secondary mirror obscuration more acceptable, thereby allowing the beam-pointing mechanism to be moved closer to the primary mirror. This arrangement also increases pointing capability in both east and west directions.

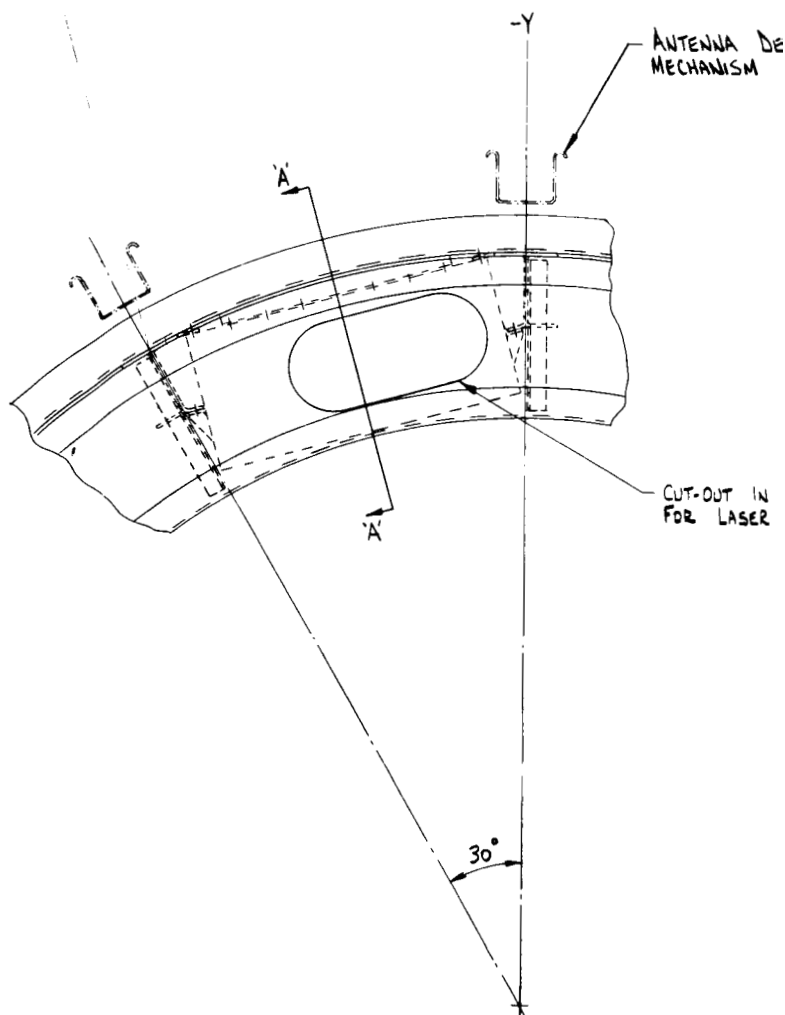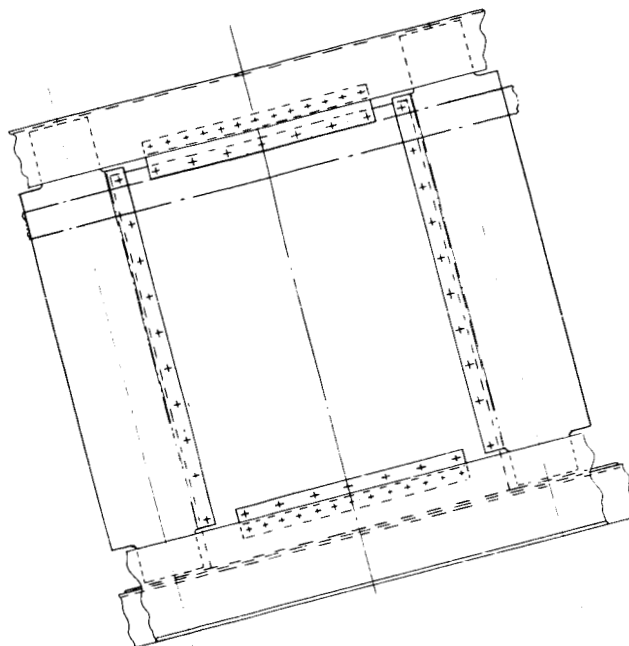## 3.4.3 PACKAGING CONSIDERATIONS

It is desirable to package the laser optical components and radiation cooler in a single modular assembly, permitting close tolerance, relative alignment of critical components, and convenient subsystem qualification and checkout. Maximum permissible dimensions of the experiment module are 22 by 17 by 7-3/4 inches. Figure 16 shows a representative installation of such an experiment package in the aft module. The parabolic-antenna components shown are based on the Goodyear Aerospace breadboard model now in production; structural details are typical.

To suit the synchronous orbit, the heat-rejection area must be restricted to the external sidewall of the module. The concept shown requires installation and removal of the package from the adapter side of the aft module to optimize the available space. Radial accessibility, presently requested by ATS for all electronics, may be achieved if later analyses show that package dimensions can be reduced.

Thermal-control requirements and volume limitations make it desirable to separate the drive, laser stabilization, and signal-processing electronics from the optical portion of the experiment and mount them separately in the adjoining equipment bay. These electronics lend themselves to packaging in standard modules, such as the 6 by 8 by 6.5-inch modules designated in the call for experiments. The estimated volume of these components is 280 cubic inches, requiring one such module. The laser and reflector components can be packaged in any of several alternate arrangements (Figures 17 and 18). One primary consideration is locating the radiation cooler near the center of the thermal radiating panel, in order to minimize blockage of the radiating area from spacecraft protrusions and still maintain sufficient and separate radiation area for the lasers.

The radiation cooler shown in Figure 16 is a staged radiator designed particularly to decouple the detectors from the spacecraft environment. Existing

34

-Y

ANTENNA DE
MECHANISM

'A'

'A'

CUT-OUT IN
FOR LASER

30°

ANTENNA CHAIN DRIVE.

ANTENNA INTERFACE.

RADIATION COOLER.

28 T.Hz. LASER COMMUNICATION EXPT. PACKAGE.

PART SECTION A-A

DEPLOYMENT CHANNEL.

CHANNEL FOR ANTENNA DEPLOYMENT MECHANISM.

ANTENNA INTERFACE RING.

ANTENNA CHAIN DRIVE.

AFT MODULE STRUCTURE.

AFT MODULE STRUCTURE
COMMUNICATION EXPT.
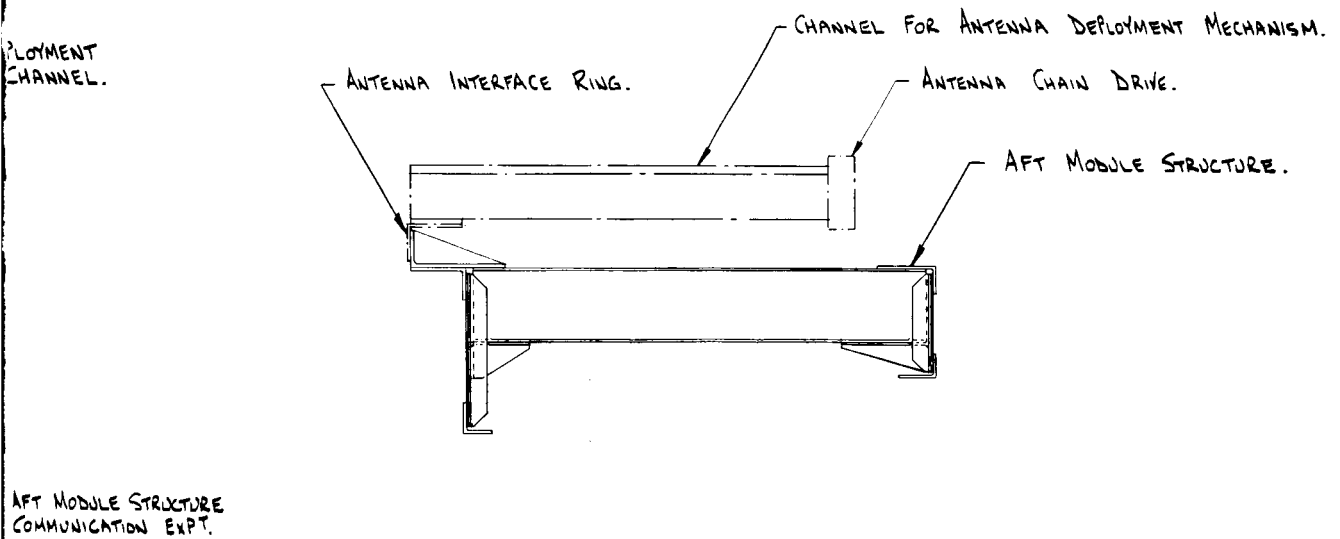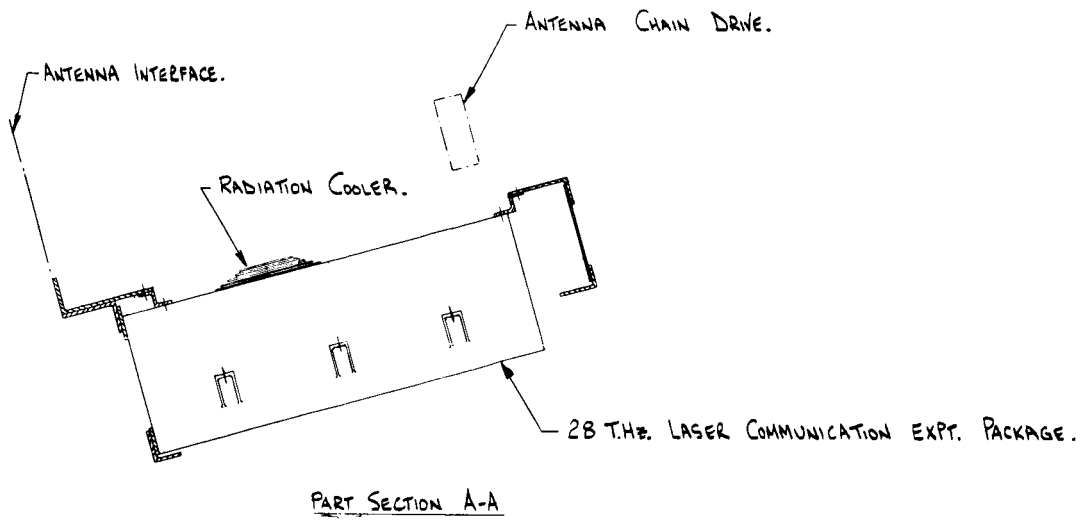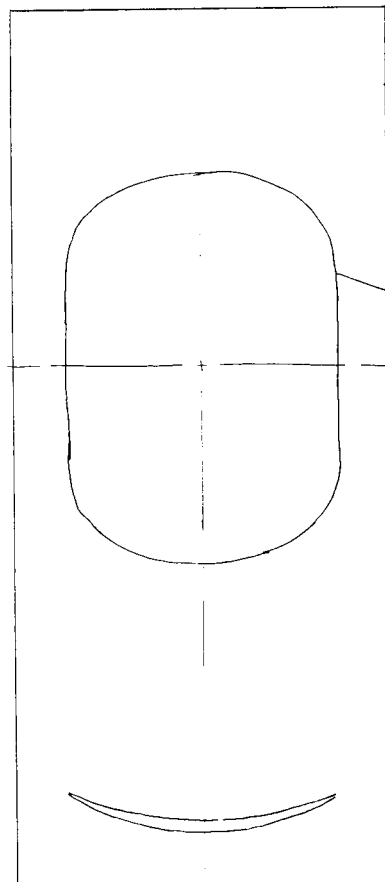
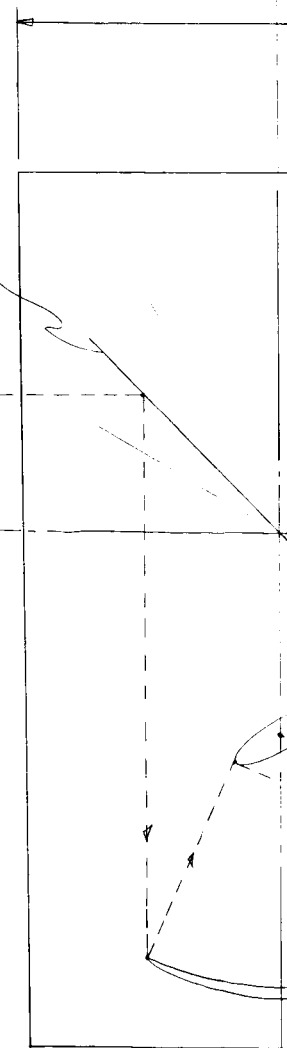Figure 16. Package Design Configuration

35

PRECEDING PAGE BLANK NOT FILMED.

MIRROR

EARTH

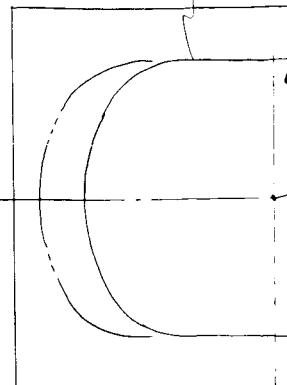MIRROR

MIRROR

EARTH
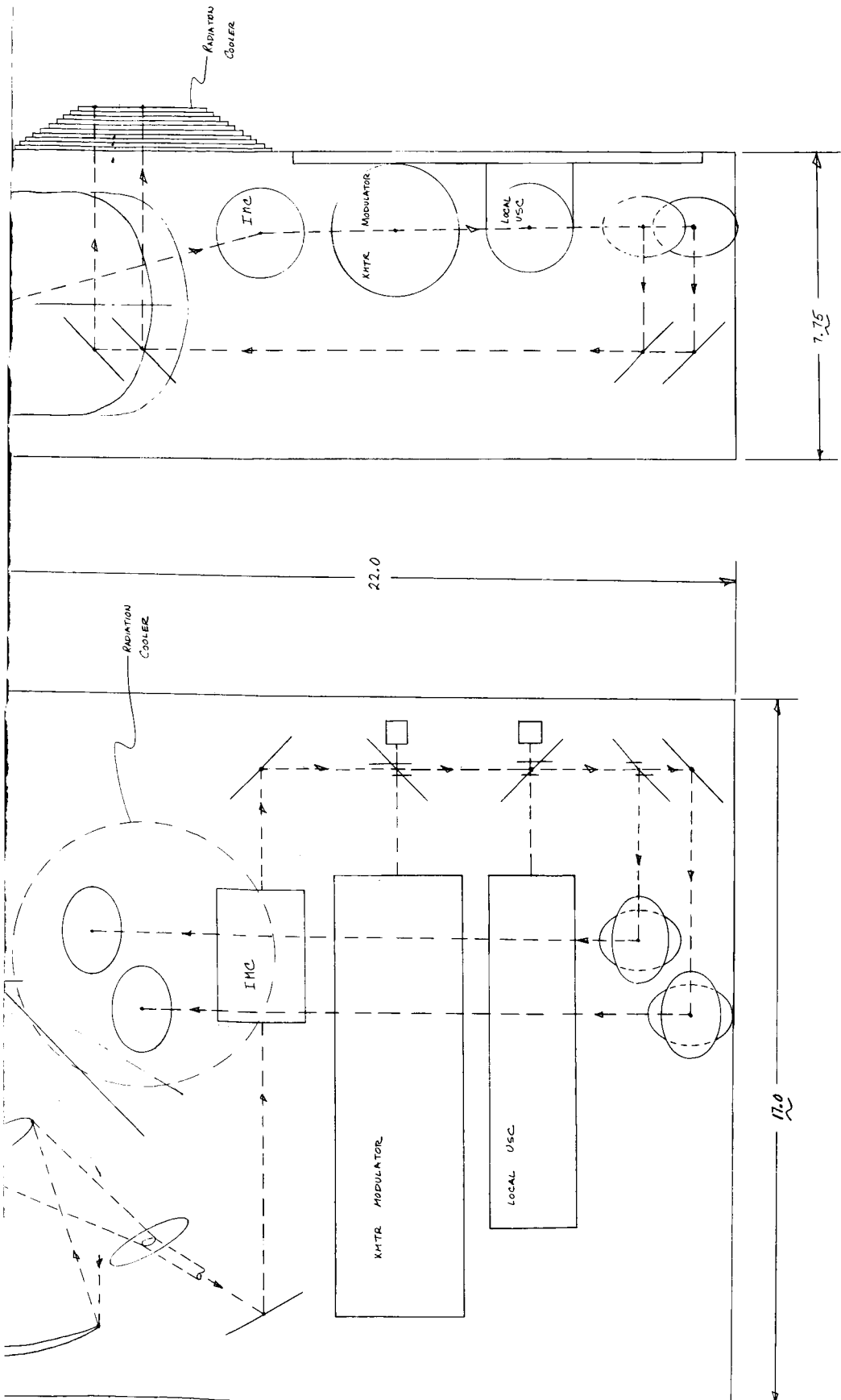
Figure 17. Component Packaging Concept
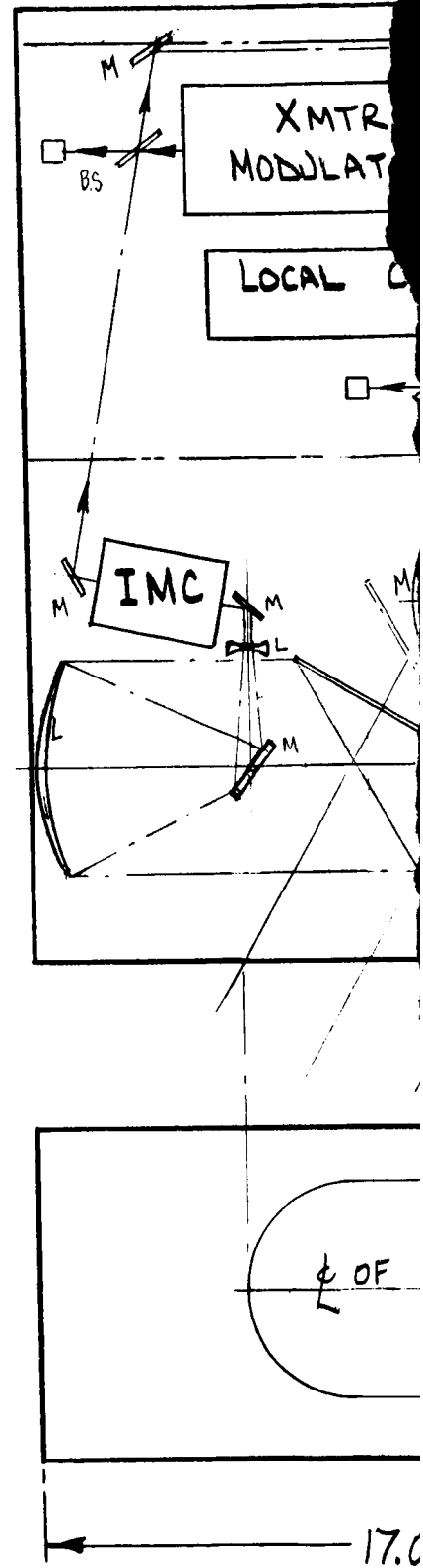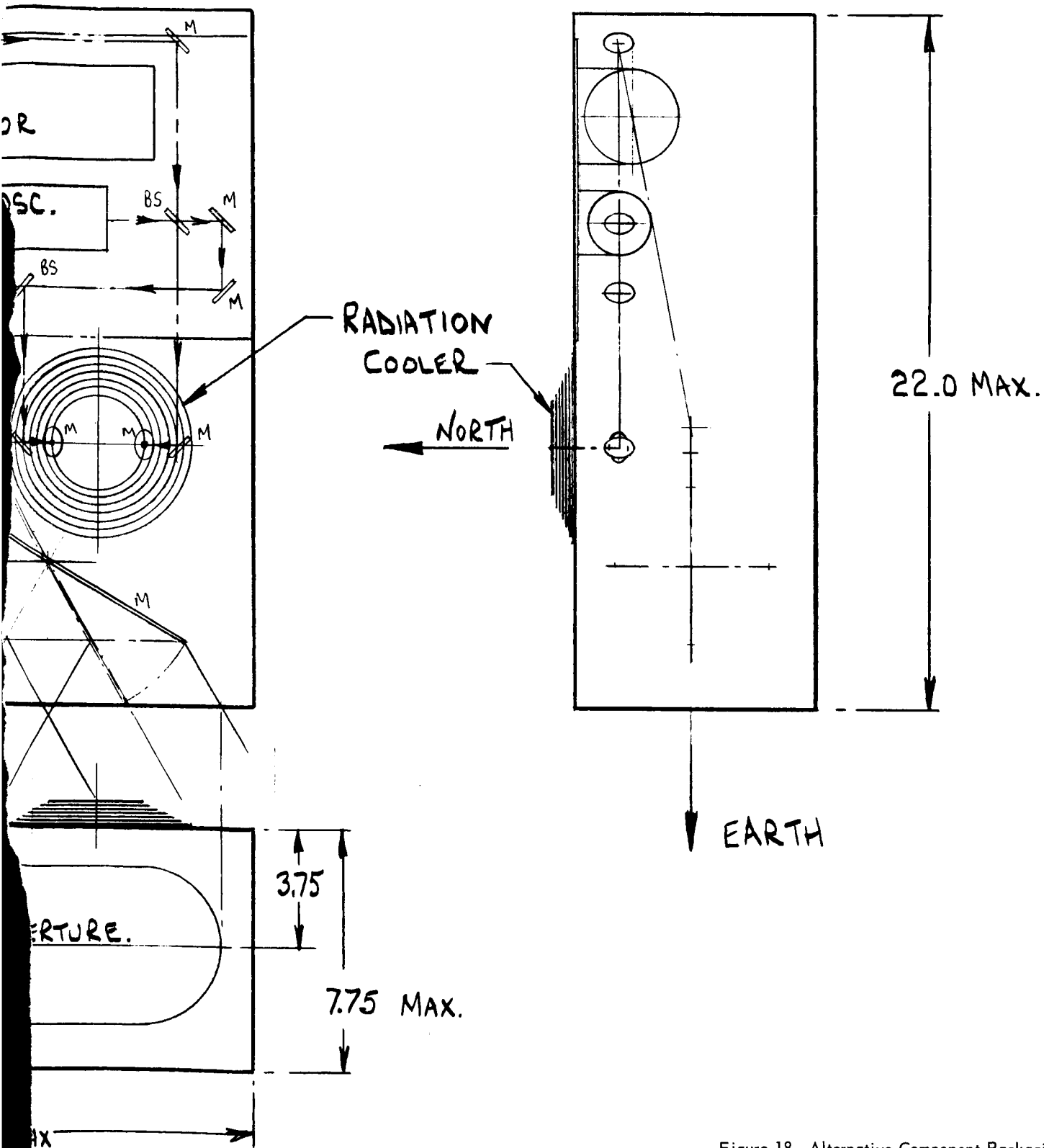
37

XMTR
MODULAT

BS

LOCAL C

M

IMC
M
M

L

L
M

L

OF

17.0

R

OSC.

BS

BS

M

RADIATION
COOLER

NORTH

22.0 MAX.

EARTH

3.75

ERTURE.

7.75 MAX.

AX

Figure 18. Alternative Component Packaging Concept

39

tunnel- or wedge-type coolers that meet the performance requirements may also be considered for this design (Reference 11). Adding sun shields will extend the duty cycle through the summer; however, reflections of the parabolic antenna on the shield will affect radiator performance, so that a shield must be designed specifically for the spacecraft.

3.5 THERMAL CONTROL

3.5.1 ELECTRONICS

The electronics (5.6-watt signal-processor electronics; 8.4-watt power-supply systems) have a total dissipation of 14 watts. This equipment will be installed in one of the aft-module equipment bays whose surface is at an angle of 15 degrees to the yaw-pitch plane. A typical shutter system installed on this bay surface has a heat-rejection capability from 11 to 25 watts/ft^2 at 25°C. With a total equipment dissipation of 14 watts, 1.3 square foot of bay louver surface is required. Since 1.67 square feet are available (18.3 watts worst-case capability), the present bay design will adequately incorporate this equipment. In a cold orbit with the shutters closed, 19.2 watts are required to maintain 25°C, and the equipment dissipates 14 watts. Therefore, this equipment can be maintained at a suitable operating temperature range with no thermal modifications to the existing bay design.

3.5.2 LASER PACKAGE

The laser package containing the optics, 5-watt transmitter module, 1-watt local oscillator, 0.01-watt image motion compensator, and five 0.002-watt detectors will be mounted in the bay adjacent to the electronics components. The laser transmitter module and the local oscillator should be maintained at a near-constant temperature level. Rather than place a difficult temperature requirement on the thermal interface, an active frequency-control element has been incorporated within the laser cavity. Upon sensing a change in laser temperature, the element appropriate voltages are applied to piezoelectric laser cavity elements, and the laser frequency is maintained.

The laser transmitter module and local oscillator will be mounted to the space-facing surface of the package. The lasers will be thermally mounted to the package surface, limiting the maximum gradient from the elements to the package surface to less than 5°C. The box will be passively controlled to reject 6.0 watts from the package surface at 20°C. For a package surface perpendicular to north-facing, the maximum heat-rejection capability during summer solstice is 12.4 watts/ft^2. With 6.0-watt dissipation, a radiator area of 0.5 square foot is required, and the remaining space-facing package surface (except for the area where the detector radiator protrudes) will be well insulated. With the

present bay design, the package surface will be at a 15-degree angle to the yaw-pitch plane and, during periods of high solar impingement, experiment operation may have to be restricted to less than 12 hours per day. However, by using a larger radiator area and suitable shadowing, it is expected that continuous operation could be maintained. Because only 500 hours of operational time are required at a rate of not more than 3 hours a day, the experiment objectives can be met with the present design.

Maintaining the five 0.002-watt detectors below 100°K with a passive radiator represents the limiting problem thermally. In order to maintain temperatures below 100°K, the radiator must be extremely well insulated from the vehicle, and can receive no direct or reflected solar energy. In addition, earth albedo as well as direct radiation from any vehicle surfaces must be eliminated. If good insulation were installed between the radiator and vehicle with plastic support mounts capable of withstanding vibration loads, an effective emissivity of 0.015 could be obtained. With this 0.015 emissivity, a vehicle temperature of 20°C, and a radiator of 77°K, 0.582 watt/ft^2 of energy would be transferred from the vehicle to the radiator. Since a radiator with an emissivity of 0.95 at 77°K has a radiation capability of only 0.18 watt/ft^2, the heat leak from the vehicle is too high to maintain the radiator temperature at 77°K, even if the detectors dissipated zero power; and there is no other source of energy that can "see" the radiator. This vehicle-insulation problem can be solved by a staged-radiator system (Figures 17 and 18) consisting of a number of circular discs with decreasing diameters, which are insulated from one another. The detector is mounted to the outer disc, which is sized to reject the detector dissipation plus the heat leak from the preceding disc. The area on the outer surface of each disc from the outside diameter to the diameter of the subsequent disc has a high emissivity, allowing the heat leak from the vehicle to the first disc to radiate from the extended disc area. Consequently, temperature of the first disc is reduced and the heat leak to the next disc is minimized. With no other external fluxes incident on this staged-radiator system, the outer detector stage (0.010 watt) will have a radius of about 3 inches at 77°K; four other stages with temperatures of about 87°K, 113°K, 158°K, and 198°K will insulate the detector sufficiently from a 294°K vehicle. The diameter of the base stage will be about 6 inches. In addition, a shield system is required to protect the entire staged-radiator system from external fluxes. For example, with no shield at the summer-solstice position and a special coating with a solar absorptivity of 0.05, a flux of 2.60 watts/ft^2 would be absorbed by the radiator, limiting its temperature to 150°K with zero dissipation and no other heat inputs. Accordingly, calculations indicate that obtaining 77°K passively at low detector powers with a practical size for the existing radiator system is feasible and that such a design would be extremely sensitive to any heat input. With a radiation capability of 0.53 watt/ft^2 at 100°K (more than double 77°K), a detector temperature level between 77°K and 100°K could result, especially if the experiment duty cycle is limited during orbits with high solar radiation on the radiator side of the vehicle.

4. OPERATIONAL GROUND EQUIPMENT

4.1 GENERAL

This section describes the operational ground equipment (OGE) required to support the proposed ATS-F and -G laser communications experiment.

The function of the OGE is to provide a self-contained mobile test facility capable of performing required performance evaluation tests of the flight laser communications experiment. In conjunction with existing ground-station facilities, the OGE will be capable of evaluating both uplink and downlink experiment performance. It will exercise and evaluate the experiment in a variety of operating modes and collect data for analysis.

Evaluation of experiment performance requires establishment of test communications with the satellite from a number of test sites (e.g., GSFC, Greenbelt, Md; Rosman, N.C.; Mojave Desert; Mount Hopkins, Calif.). Therefore, the required operational ground equipment has been collected into a mobile test facility that may be readily moved between test sites. The possibility of operating with other laboratories who wish to set up 10.6-micron receiver ground stations will be investigated.

4.2 REQUIREMENTS

In order to attain the experiment test objectives, the operational ground equipment must meet the following requirements:

- The test facility will be mobile and readily transportable to remote test sites.

- OGE will be capable of rapid setup, teardown, and transport in order to permit checkout and operation at a number of remote test sites.

- Operation will be permitted in environmental temperature conditions of -40 to +140°F; the test equipment will be protected from the effects of temperature, rain, sand, dust, and humidity.

- Capability for voice and possibly teletype communications to ATS ground stations by telephone line will be provided. This communications link will be used for test coordination.

- Provision will be made to point the ground laser transmitter/receiver unit in both azimuth and elevation to a 0.1-degree accuracy relative to the earth.

- A concrete test pad, 6 feet by 6 feet by 4 inches will be required at each site.

- Geographic location of the test pad will be by normal navigational methods.

- A protective housing (astronomical dome) will be provided to protect the laser transmitter/receiver unit from the environment.

- The test facility will provide required power, operating conditions, and control to the test transmitter and receiver.

- Equipment necessary for test transmissions, data display, data recording, and preliminary data analyses will be provided.

- Laboratory space will be provided.

- Sufficient self-check capability will be provided to ensure that the test facility is operating properly and to facilitate field maintenance.

- Maximum use will be made of support equipment in the ground station that was built up during spacecraft-package development.

4.3 DESCRIPTION

Figure 19 depicts proposed operational ground equipment and its relationship to the ATS spacecraft and an ATS ground station. The OGE consists of the following major units.

- An astronomical dome that houses the laser transmitter/receiver

- An instrumentation van containing required test instrumentation and a laboratory working area

- Mobile power-generation equipment

4.3.1 ASTRONOMICAL DOME

The astronomical dome will be commercially available unit, approximately 6 feet in diameter, containing the laser transmitter/receiver package. This package, in general, is identical to the satellite experiment package. The dome mounts on a platform that is manually adjusted in azimuth and elevation to an accuracy of 0.1 degree. Boresight equipment is also located on the platform. The dome top does not need to share the same truck with the laser platform as is conventional for laser-tracking systems of earth-orbiting satellites.
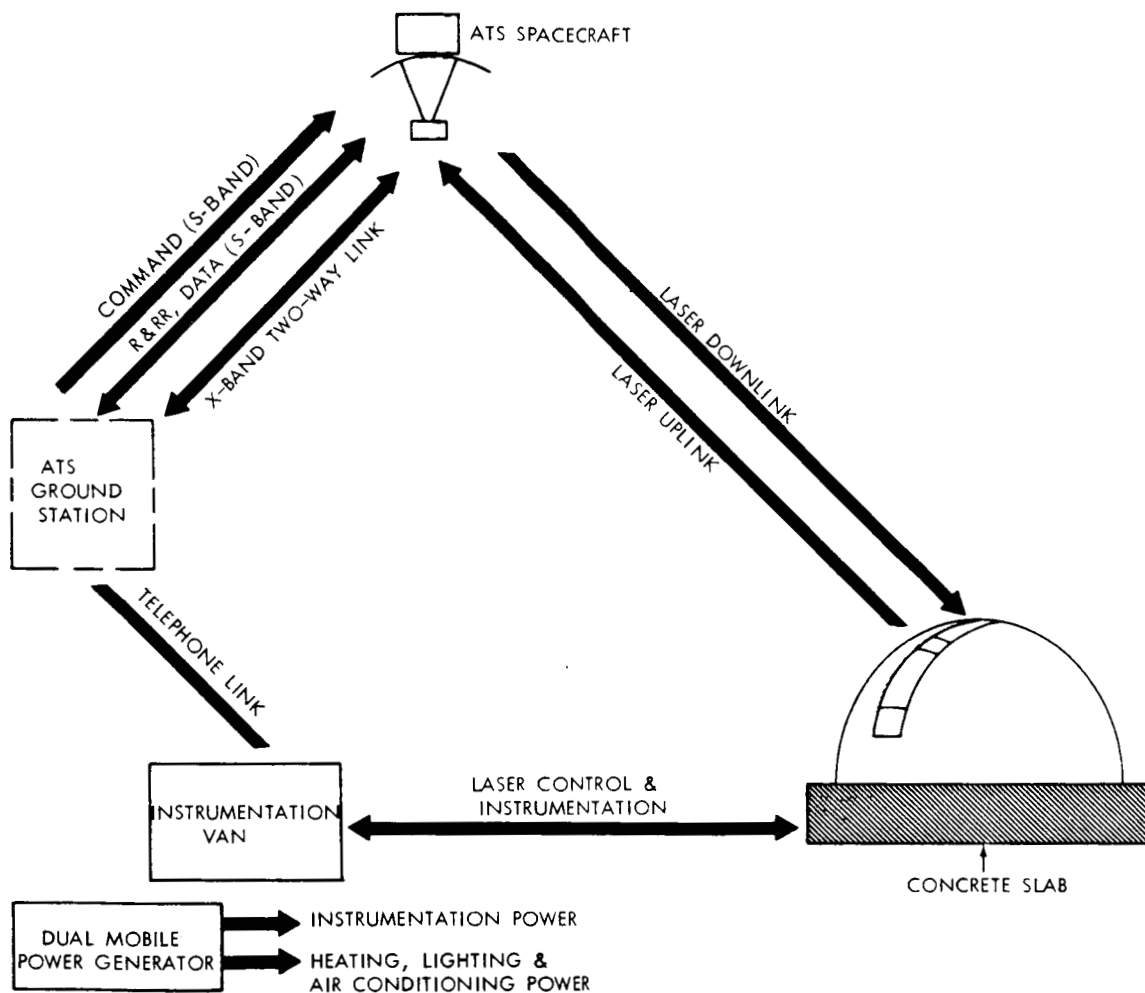
Figure 19. Ground Instrumentation Interface

A movable slit 5 inches wide will be provided for the receiver telescope. The dome and laser mout will be accurately positioned on the concrete slab site by adjustable mounting feet using precise spirit levels. Verification of position will be accomplished by bore-sighting on appropriate celestial bodies. Sufficient room will be available for an operator to turn the mount and accomplish required alignment functions. An electrical interface panel will provide all necessary power, control, and interconnection functions.

The dome will be capable of being trailer-transported; sensitive instruments will be removed from the done during transport and stowed in the instrument van. The dome-transport trailer will also transport special operating supplies such as liquid nitrogen tanks.

4.3.2 INSTRUMENTATION VAN

The instrumentation van (Figure 20) is divided into two areas: an experiment operational area, and a laboratory work area.

The instrumentation van will be between 30 and 40 feet long, 8 feet wide, and 12.5 feet high. It will be capable of being towed at speeds up to 60 mph over level concrete and macadam roads by a tow vehicle having a standard fifth-wheel assembly. The van will be equipped with cooling, heating, and humidity-control equipment capable of maintaining a suitable environment for equipment and personnel. Separate circuits will be provided for lighting, heating, cooling, and instrumentation. Mechanical supports and restraints will be provided for the optical and electronic equipment to prevent damage from road shocks during transportation.

The experiment operational area also includes:

● Meteorological équipment to measure wind speed and direction, barometric pressure, temperature, and relative humidity

CURB SIDE
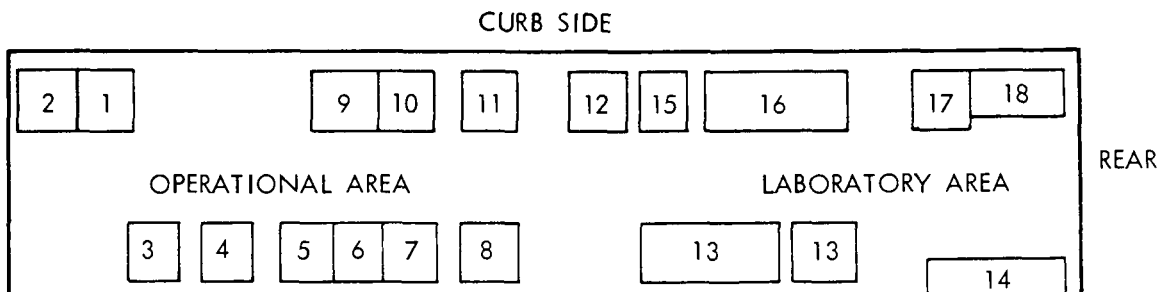
OPERATIONS AREA		LABORATORY AREA
1. LASER CONTROL		13. OPTICAL BENCH & WORK BENCH
2. STORAGE CABINET (SPARES, ETC.)		14. PWR DIST PANEL
3. TELEPRINTER		15. TEST EQUIPMENT
4. VIDEOMONITOR		16. DESK
5. EXPERIMENT CONTROL		17. TEST EQUIPMENT
6. EXPERIMENT CONTROL		18. STORAGE CABINET
7. POWER INTRUMENTATION & MONITOR		
8. COMMUNICATIONS LINK, VOICE		
9. VIDEO TAPE RECORDER		
10. VIDEO TAPE RECORDER		
11. METEOROLOGICAL INSTRUMENT RACK		
12. AIR DUCTS		

Figure 20. Instrumentation Van

- A digital computer with punched-tape input and teleprinter input/output to establish tracking information and related experiment computations

- A magnetic video tape recorder to record the signal received from the satellite and generate the signal transmitted to the satellite from a prerecorded test tape

- A video monitor to provide real-time operational display of transmitted and received signal

- Readouts for angle positions of the beam-slewing mirror, identical to the one on the satellite

- A digital clock periodically synchronized to an ATS ground station to establish experiment time reference

- Display of all parametric data monitored on the satellite unit

An optical bench in the laboratory area provides necessary alignment-check capability. Specially designed RF equipment and 10.6-micron lasers, constituting laser test receivers, will be part of the laboratory equipment. This equipment, similar to that used in the development laboratory, will be modified as necessary to facilitate field experimental use.

4.3.3 MOBILE POWER GENERATOR

A mobile level-power generator, diesel- or gasoline-operated, is required to operate the equipment at remote sites. Each section should be capable of supplying 25-kw 3-phase 208/120-volt 60-Hz power. The output from one section would supply instrumentation power; the second section would provide heating, lighting, and cooling power.

5. TELEMETRY AND COMMAND INTERFACE

5.1 TELEMETRY

The ATS-F and -G telemetry subsystem will be capable of transmitting up to 1000 channels of data. The normal in-orbit data rate will be 400 10-bit samples per second. The data processor, capable of handling 10-bit accuracy, will accept as inputs analog signals, 10-bit serial digital signals, and single-bit signals. The analog inputs will be digitized by an 8-bit analog-to-digital converter.

Telemetry requirements for this experiment (Table 3) will consist of 22 to 24 analog signals, six single-bit (on-off) signals, and two 10-bit serial digital words.

Table 3
Tentative Telemetry Data Requirements

Parameter	Quantity	Type
Thermopile power	2	A
Laser mirror piezoelectric crystal voltage	2	A
IMC tracking logs error	2	A
Voltage monitor	12	A
Temperature monitor	5	A
Mirror position	2	D (10-bit serial)
Local oscillator	1	D (1-bit)
IMC	1	D (1-bit)
Laser carrier	1	D (1-bit)
Modulator	1	D (1-bit)
Position of tuning switch	1	A
Position of modulation index switch (optional)	1	A
Position of LO voltage switch (optional)	1	A
Laser-X-band cross strap	1	D (1-bit)
X-band-laser cross strap	1	D (1-bit)

5.2 COMMAND

The ATS-F and -G command subsystem will be capable of accepting and executing two types of commands: switching commands will be processed to an X-Y matrix providing 256 outputs, and digital work commands of 10-bit length will be addressed to 12 locations.

This experiment can be implemented to use the spacecraft command capability in several ways, depending on the availability of switching commands and digital word commands. Six switching commands would be required to energize the experiment equipment in the proper sequence, and a single reset command can return the equipment to the de-energized state.

Mirror position control can be achieved by digital word commands for each degree of freedom (azimuth and elevation). The position precision required indicates the need for a 10-bit command word. This can be provided by inserting a position command into a buffer register in two 6-bit groups and then commanding readout to either the azimuth or elevation mirror controller by use of either of two switching commands.

Several methods may be used to tune the transmitter carrier frequency to any one of five points within any one of five discrete bands. For example, either of the following approaches would accomplish the required tuning:

- A digital word command would set the desired number of incremental steps of a switch.

- A discrete switching command would increment a switch one step at a time by ground command. A plus and a minus step command could be provided to halve the time required to reach any desired switch position.

Either approach could be used for local oscillator voltage selection (one of four) or for modulation index selection (one of five). Also, discrete switching commands may be used to select the appropriate circuit elements.

Command requirements are:

Local oscillator ON	Discrete
Image-motion compensator scan ON	Discrete
Laser transmitter carrier ON	Discrete
Modulator ON	Discrete
Laser to X-band cross-strap	Discrete
X-band to laser cross-strap	Discrete
Experiment OFF	Discrete

49

Mirror position	10 bits
Readout mirror position, azimuth	Discrete
Readout mirror position, elevation	Discrete
Tune transmitter frequency	1 of 25 positions
Select local oscillator voltage	1 of 4 positions
Select modulation index	1 of 5 positions

5.3 CONTROL SEQUENCES

Control sequences for the two experiments appear in the following paragraphs. (Steps in parentheses are performed on the ground and do not require command or telemetry.)

5.3.1 FIRST EXPERIMENT

1. Command

   Turn on LO and adjust voltage to either

   (a) 320 volts
   (b) 325 volts
   (c) 327 volts
   (d) 330 volts

2a. Read power on thermopile

2b. Telemetry — thermopile power

   5 bits   10 minutes between readings

3a. Read LO temperature

3b. Telemetry

   5 bits   10 minutes between readings

4a. Read LO mirror piezoelectric crystal voltage

4b. Telemetry

   5 bits   10 minutes between readings

5a. Command/control

   5-inch mirror slew

   Position mirror in azimuth–10 bits
                   in elevation–10 bits

5b. Telemetry

   Read mirror position (pick-off)

   Azimuth 10 bits

   Elevation 10 bits

  6. (Turn on ground laser beacon)

  7. Command

   Turn on image motion compensator (IMC) scan

  8. Read IMC tracking loop error signal

8a. Telemetry

   IMC tracking loop error signal–

   5 bits in each of two axes

  9. (Turn on ground video laser experiment)

10a. Command LO mirror piezoelectric crystal voltage verification

11a. Command

   Laser transmitter on ATS-F to turn on carrier

11b. Telemetry

   Verification of 9A

12a. Thermopile reading

12b. Telemetry

Read thermopile

5 bits   10 minutes between readings

13. (Lock to transmitter signal with ground receiver and point laser)

14. Command

Tune transmitter carrier frequency—5 discrete bands 5 bits

15. Command

Turn on modulator and command 3 bits for modulation index

16. Command

X-band to laser cross-strap

17. (Turn on X-band ATS-F experiment—use telephone request and transmit color TV tape image over video link to X-band experimental van)

18. (Modulate X-band uplink with video tape image)

19. (Demodulate image on ATS-F and feed to laser modulator)

20. (Record demodulated laser signal on ground)

5.3.2 SECOND EXPERIMENT

21. Repeat steps 1 through 15

22. Command

Laser to X-band cross-strap

23. (Modulate ground laser transmitter with color video image)

24. (Record demodulated X-band ground video)

25. Monitor points

7 voltage points	4 bits each at drift rates
3 voltage points	5 bits each at drift rates
2 voltage points	2 bits each at drift rates
2 points	5 bits each at drift rates
3 points	3 bits each at drift rates

6. DATA ANALYSIS

It is premature to describe details of data analysis and processing for a co-operative microwave-laser experiment such as the one described in Figure 2. We confine our explanation to the Phase 1 experiments (i.e., the transmission of test video tapes between ATS-F and the OGE, and the relay of this video signal from ATS-F to the STADAN control via the X-band experiment). Two identical pairs of test video tapes will be cut at Goddard Space Flight Center; one pair will be mailed to STADAN control, the other sent to the OGE. During the experiment, two video tapes will be duplexed onto the outer extremities of the OGE laser modulator's baseband.

The video data transmission quality will be recorded on tapes at the receiver stations. Separate "housekeeping" tapes will also be generated to provide information on experiment-component performance as well as on satellite performance (laser transmitter-carrier power, commands given to the flight package, relative humidity at the OGE, image-motion compensator error signal, reading from vibration-pickup head on the OGE laser head, laser modulator drive voltage, and satellite control and power supply performance data).

Six tapes constitute the raw data for one experiment session. A session lasts approximately 3 hours. The six tapes are:

- The audio tape cut at the OGE

- Two video tapes cut at GSFC which are imposed on the laser modulator at the OGE

- Two video tapes which are demodulated from the X-band receiver or the laser receiver on the ground

- An audio tape cut at the X-band receiver which records the peripheral information at the X-band experimental ground-station control

The 3-hour experimental session is divided into three-sections:

- Approximately two hours of laser warm-up and tuning preparation

- Approximately one-half hour of video transmission

- Approximately one-half hour of miscellaneous experiments (such as receiving background noise on the ATS-F laser receiver while tuning the receiver over its entire band)

7. RELIABILITY

Most of the components and subsystems used in this experiment are readily available in space-qualified form and they, or their equivalents, have been successfully flown on numerous space missions. Two areas, however, deserve special attention: the CO_2 lasers, and the coarse beam-pointing mechanism.

In order to guarantee the estimated 500-hour operating life needed by the on-board CO_2 laser systems, a conservative requirement of at least 1000 operating hours can be demanded. Such a requirement is well within the current state-of-the-art for CO_2 lasers, although care must be taken with regard to gas additives, electrode materials, and discharge tube processing and material. Laser systems satisfying the requirement of at least a 1000-hour operating lifetime have been described by Witteman (References 12 and 13) and Carbone (References 14 and 15). In addition to the operating lifetime requirements, it is also necessary to ensure that the lasers can withstand the vibration environment encountered during launch. Recently constructed CO_2 lasers, such as the one shown in Figure III-15 (see also Reference 16), which employ Cervit yokes to support the laser tube, appear to have no limitations which would bar the construction of a space-qualified, ruggedized laser system.

The aspect of the coarse beam-pointing mechanism (the only moving part in the system) which deserves special attention is lubrication. Although successful completion of this experiment requires achievement of an operating lifetime well in excess of one year, the problems of retaining adequate lubrication in a space environment for so long a period have been encountered in previous space missions and have been largely solved. A very similar system is described in Reference 17, which discusses a day/night meteorological camera subsystem for ATS-D. This system had requirements more stringent than those placed on the experiment described in this document.

A study program made by Hazeltine Corp. for Goddard Space Flight Center (Reference 18) on ball-bearing lubrication for Nimbus-D and ATS-D camera

54

mechanisms offers one possible solution. The conclusion of the study is given below:

A dry laminar lubricant, molybdenum disulfide, should be used for lubricating NIMBUS and ATS camera ball bearings. A glass-filled teflon ball retainer should be used. The lubricant should be applied to the balls and retainer but not to the races. Ball-bearing shields should be provided on the bearing to keep dust out, and as a radiation and micrometeorite shield. The shields will also act to impede migration of silicone oils or other contaminants in a vacuum environment. A 1/8-inch-thick magnesium alley cover should be provided in the design to attenuate radiation dosage to the teflon ball-bearing retainer.

This discussion indicates that lubrication of the coarse beam-pointing mechanism is a problem which can be solved with readily available state-of-the-art technology.

REFERENCES

1. Goodwin, F. E., and Nussmeier, T. A.: Optical Heterodyne Experiments at 10.6 Microns. Paper 10J-5 presented at the 1968 International Quantum Electronics Conference, Miami, Fla., May 14-17, 1968

2. Long Range Network Capability Plan Tracking and Data Systems. Goddard Space Flight Center, October, 1966

3. Wolfe, W. L. (editor): Handbook of Military Infrared Technology. U. S. Government Printing Office, 1965, p. 353

4. Parker, R. N.: Optical Beam Steering Device. Final Report on Contract NAS-5-9688, North American Aviation, Inc., Autonetics Division, 18 Jan. 1967

5. Mocker, H. W.: Rotational Level Competition in CO_2 Lasers. Paper 7G-6 presented at the 1968 International Quantum Electronics Conference, Miami, Fla., May 14-17, 1968

6. Operations Manual for Experimental CO_2 Laser Model 947B. Manual included with laser system fabricated under Contract NAS-5-10309. Sylvania Electronic Systems, Western Division, Mountain View, Calif., 1968

7. Taming the CO_2 Laser. Electronics, Vol. 41, No. 8, Apr. 15, 1968, pp. 54-56

8. Arams, F., Peyton, B., Sard, E., and Pace, F.: Final Report for High-Sensitivity Infrared Receiver Development. Contract NAS-5-10156, July, 1967

10. The Honeywell Radiation Center.: A Laser Communications Experiment. Document No. 84-15. Honeywell Inc., Radiation Center, Boston, Mass., 1968

11. Annable, R. V., Lodder, J. F., Harber, R. A., and Leiter, H. A.: Final Report for a Day-Night High Resolution Infrared Radiometer Employing Two-Stage Radiant Cooling. Contract NAS-5-10113, 11 Dec. 1967

12. Witteman, W. J.: Sealed-off High Power CO_2 Lasers. Phillips Technical Review, Vol. 28, No. 10, Oct. 1967, pp. 287-296

13. Witteman, W. J.: High Output Powers and Long Lifetimes of Sealed-Off CO_2 Lasers. Appl. Phys. Lett., Vol. 11, Dec. 1, 1967, pp. 337-338

14. Carbone, R. J.: Long-Term Operation of a Sealed CO_2 Laser. IEEE J. Quantum Electronics, Vol. QE-3, No. 9, Sept. 1967, pp. 373-375

15. Carbone, R. J.: Continuous Operation of a Long-Lived CO_2 Laser Tube. IEEE J. Quantum Electronics, Vol. QE-4, No. 3, Mar. 1968, pp. 102-103

16. Mocker, H. W.: 10.6 Micron Optical Heterodyne Communication System. Phase 3 Report for period 1 August through 31 Oct. 1967 on Contract NAS-8-20645. Honeywell Inc., Systems & Research Department, Minneapolis, Minn., 31 Oct. 1967

17. Hazeltine Corporation: Combined Quarterly and Study Report for Applications Technology Satellite (ATS-D) Day-Night Meteorological Camera Subsystem. 1966 July 1 to 1966 Nov. 2. Contract NAS-5-9605. Hazeltine Corp., Little Neck, N.Y.

18. Hazeltine Corporation: Study Program of Ball Bearing Lubrication for Nimbus-D and ATS-D Camera Mechanisms. Appendix H of Hazeltine Corp. Report 10237. Hazeltine Corp., Little Neck, N.Y.

APPENDIX

RANGE-SIGNAL CALCULATIONS

The power received by a receiver whose antenna intercepts a solid angle $\Delta\Omega r$ from the transmitter is

$$P_r = \frac{dP_T}{d\Omega_T} \Delta\Omega_r \qquad (1)$$

where $dP/d\Omega_T$ is the watts per steradian emitted from the transmitter in the direction of the receiver. Equation (1) assumes that $\Delta\Omega_r$ is sufficiently small that $dP/d\Omega_T$ is uniform over the receiver antenna. This is always the case in the far-field pattern. We rewrite equation (1) as

$$P_r = P_T \left(4\pi \frac{dp}{d\Omega_T} \right) \frac{\Delta\Omega_r}{4\pi} , \qquad (2)$$

where

$$\frac{dp}{d\Omega_T} \equiv \frac{dP}{P_T d\Omega_T} . \qquad (3)$$

P_T is total transmitted power; p is fractional power.

Substituting into equation (2) the receiver area, A_r, and range for $\Delta\Omega_r$, we have

$$P_r = P_T \left(4\pi \frac{dp}{d\Omega_T} \right) \frac{A_r}{4\pi R^2} . \qquad (4)$$

Antenna gain is defined as

$$G = 4\pi \frac{dp}{d\Omega} . \qquad (5)$$

Note that for an isotropic radiator the gain is

$$G = 4\pi \left(\frac{1}{4\pi}\right) = 1.$$

Equations (4) and (5) give

$$P_r = P_T \frac{G_T A_r}{4\pi R^2}. \tag{6}$$

We wish now to find an expression for receiver gain as a function of wavelength and receiver aperture area; i.e.,

$$G_r = f(A_r, \lambda). \tag{7}$$

The explicate equation for G_r will depend on the distribution of intensity of the radiation illuminating the antenna. We will assume a Gaussian distribution, because experimentation has shown the intensity distribution of single-mode CO_2 lasers operating in the TEM_{00q} mode to be very close to Gaussian (see Figure A-2).

The Gaussian distribution expression is

$$I(r) = \frac{2P_T}{\pi a^2} \epsilon^{\frac{-2r^2}{a^2}} \tag{8}$$

As given in Figure A-1, r is the radial distance at which the intensity is measured; a is the radial distance at which I decreases to $1/\epsilon^2$ of its value for $r = 0$.

We shall assume that the antenna aperture is of radius a and that the edge defraction imposes very small far-field effects.

From Huygen's integral equation, it can be shown that the far-field distribution of the radiation is also Gaussian; i.e.,

$$I = \frac{2P_0}{\pi a'^2} \epsilon^{\frac{-2r'^2}{a'^2}} \tag{9}$$
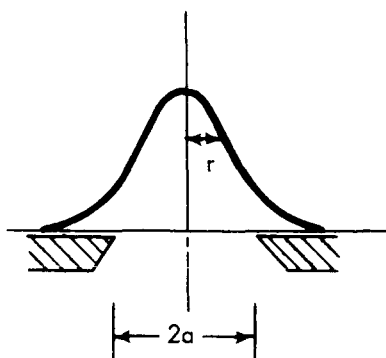
58

Figure A-1 — Gaussian Intensity
Distribution of Radiation From an
Aperture as a Function of Aper-
ture Radius.

where a' is the radius at which the radiation falls off to $1/\epsilon^2$ of the value at $r = 0$. Figure A-3 represents the r' coordinate system.

The vital relation required for calculating antenna gain is the connection between a and a' which is[1]

$$a' = \frac{R\lambda}{\pi a}.$$ (10)

where λ is the wavelength of radiation and R is the range at which I is measured. Thus the radiation intensity at a range R from an aperture diameter $2a$, illuminated by total power P_0 in a Gaussian intensity distribution, is

$$I = \frac{2P_0}{\pi a'^2} \epsilon^{\frac{-2r'^2}{a'^2}}$$ (11)

where

$$a' = \frac{R\lambda}{\pi a}.$$

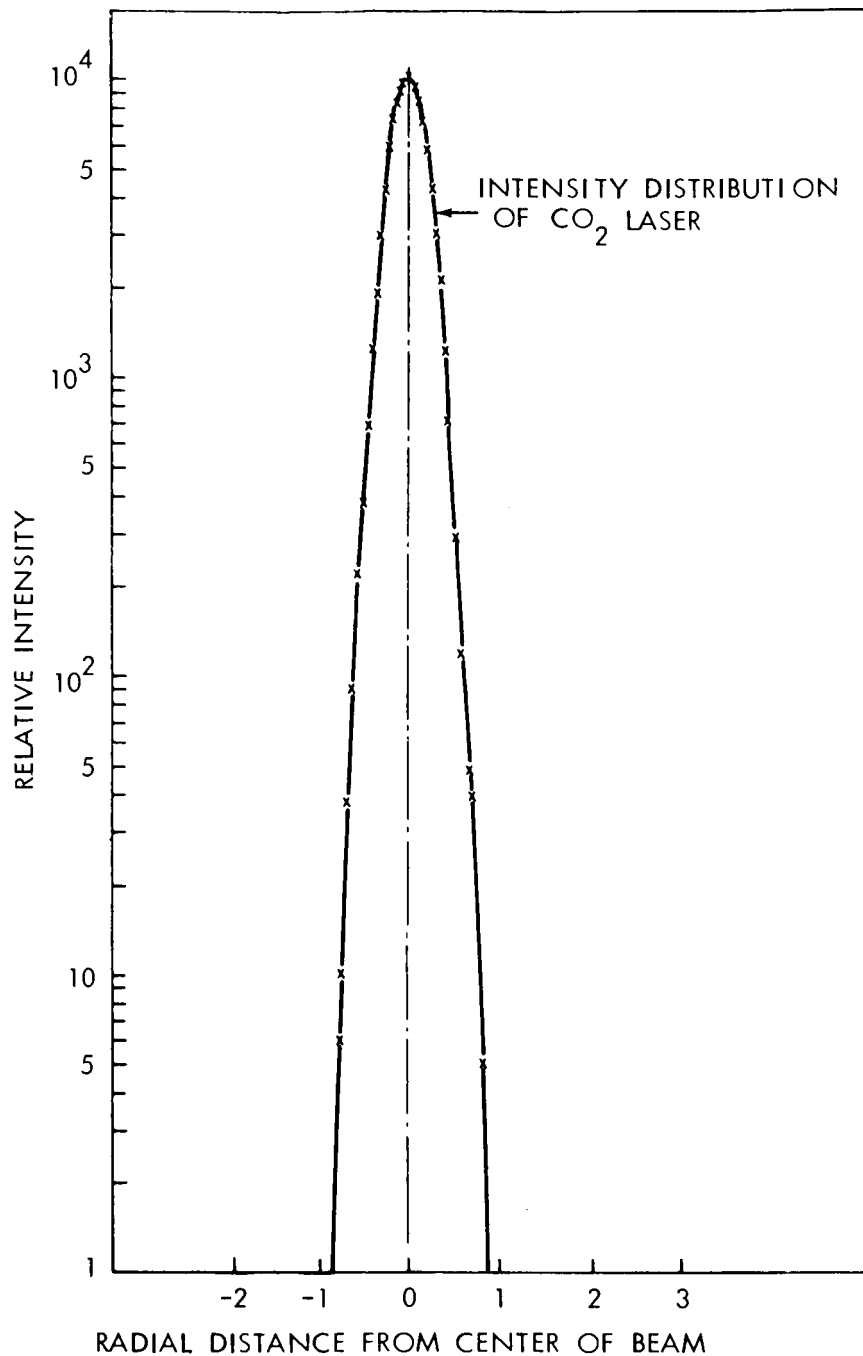[1]"Laser Technology Bulletin," No. 5; Spectra-Physics, Inc., Mountain View, California. 1966

Figure A-2—Graph of $\overline{I} = \overline{E} \times \overline{H} = \dfrac{2P_0}{\pi a^2} \, \epsilon^{\frac{-2r^2}{a^2}}$, the Gaussian Intensity Distribution (Unpublished data supplied by H. Mocker of Honeywell Inc.)
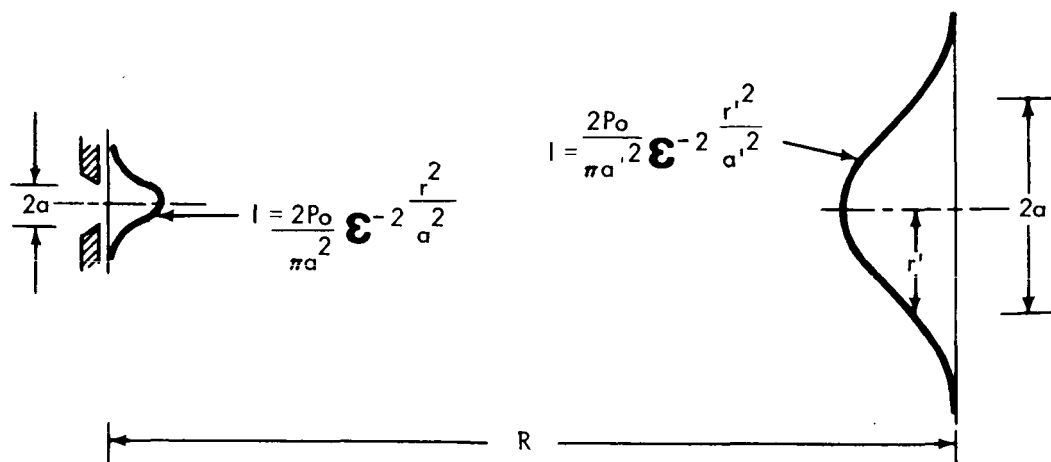
Figure A-3—Far-field Pattern of Aperture with Gaussian Intensity Distribution

In terms of radiation per unit solid angle Ω at range R, equation (11) becomes

$$\frac{dP}{d\Omega} = \frac{2P_0}{\Omega_0} \, \epsilon^{-\frac{2\Omega}{\Omega_0}} \tag{12}$$

where Ω_0 is the solid angles at whose boundary the intensity, I, has fallen off by $1/\epsilon^2$ of the maximum value.

Quantitatively,

$$\Omega_0 = \frac{\pi a'^2}{R^2} . \tag{13}$$

For $\Omega = 0$, the maximum value for $dP/d\Omega$ in equation (12) is

$$\frac{dP}{d\Omega}\bigg|_{\Omega = 0} = \frac{2P_0}{\Omega_0} . \tag{14}$$

We assume that the antenna are sufficiently well pointed to ensure that

$$\frac{dP}{d\Omega} = \frac{dP}{d\Omega}\bigg|_{max} . \tag{15}$$

61

Equations (5) and (14) give for the maximum antenna gain,

$$G_{max} = \frac{4\pi}{P_0}\left(\frac{2P_0}{\Omega_0}\right), \tag{16}$$

or

$$G_{max} = \frac{8\pi}{\Omega_0}. \tag{17}$$

To put G_{max} in terms of wavelength and receiver area, we substitute equations (13) and (10) into equation (17), giving

$$G_{max} = \frac{8\pi A}{\lambda^2}. \tag{18}$$

We have established that, if an antenna with an aperture of area A is illuminated with radiation of a Gaussian intensity distribution, and if the radiation intensity has fallen off by $1/\epsilon^2$ at the circular aperture edge, the maximum antenna gain is given by equation (18).

Substituting equation (18), the receiver antenna gain, into the range equation (6), we obtain for the range equation

$$P_r = \frac{\frac{1}{2}P_T G_T G_r \lambda^2}{(4\pi R)^2}.$$

This is the range equation (except for the 1/2 factor) given in "Reference Data for Radio Engineers," International Telephone and Telegraph Corporation, 67 Broad Street, New York, 1957, p. 676; equation (16).

For calculation of range equation for a 10.6-micron system between ATS-F and ground, we assume:

$$P_r = \frac{1}{2}P_t \frac{G_T G_r \lambda^2}{(4\pi R)^2}$$

$$P_T = 0.4 \text{ watts}$$

$$\text{Antenna aperture} = 5 \text{ inches}$$

$$G = 8\pi A / \lambda^2$$

$$R = 3 \times 10^7 \text{ M}.$$

We obtain

$$G = \frac{8\pi \, (\pi \times .127^2) \text{ M}^2}{(1.06 \times 10^{-5})^2 \text{ M}^2}$$

$$G = 1.13 \times 10^{10} \ (= 100.56 \text{ db})$$

$$P_r = \frac{\frac{1}{2}(.4) \ [(1.28) \times 10^{20}] \ [1.12 \times 10^{-10}]}{[12\pi \times 10^7]^2}$$

$$P_r = 2.2 \times 10^{-8} \text{ watts}.$$

10-db total degradation due to atmosphere and optical loss give power at the mixer as

$$P_r = 2.2 \times 10^{-9} \text{ watts}.$$

With a minimum detectable signal per cycle bandwidth at the receiver of

$$NEP = 10^{-19} \text{ watts},$$

and a 30-MHz bandwidth, we get a signal-to-noise ratio of

$$\frac{S}{N} = \frac{2.2 \times 10^{-9}}{10^{-19} \times 3.3 \times 10^7} = 6.7 \times 10^2, \text{ or } 28.3 \text{ db}.$$

SYMBOLS

a, a′	radial distance at which power falls off to $1/\epsilon^2$ of its maximum value for Gaussian distribution
A	antenna area
A_r	receiver antenna area
ϵ	2.712
E	electric field
f	function of
G	antenna gain
G_r	receiver antenna gain
G_T	transmitter antenna gain
H	magnetic field
I	power per unit area
NEP	noise equivalent power
p	fractional power
P	power
P_r	power received
P_T	transmitted power
i, r	antenna radius
R	distance between transmitter and receiver
S/N	signal-to-noise power ratio
$\Delta\Omega$	solid angle subtended by receiver antenna
λ	wavelength of radiation
π	3.1416
Ω	solid angle
Ω_T	solid angle subtended by transmitted beam